Marine and Petroleum Geology
June 2015, Volume 64, Pages 76-103
http://dx.doi.org/10.1016/j.marpetgeo.2014.12.015
http://archimer.ifremer.fr/doc/00252/36373/

Tectonics and sedimentation interactions in the east Caribbean subduction zone: An overview from the Orinoco delta and the Barbados accretionary prism

Deville Eric [1,*], Mascle A. [1], Callec Y. [1], Huyghe P. [2], Lallemant S. [3], Lerat O. [1], Mathieu X. [4], Padron De Carillo C. [1,2], Patriat Martin [5], Pichot Thibaud [5], Loubrieux B. [5], Granjeon D. [1]

[1] IFP School-IFPEN, 1-4 avenue du Bois Préau. 92852 Rueil-Malmaison Cedex. France
[2] Université Joseph Fourier, 38041 Grenoble Cedex. France
[3] Université de Cergy-Pontoise, av. du parc, 95031 Cergy-Pontoise, France
[4] TOTAL E&P China, Chang' an Metropolis Center Room 905-906 Floor9, Building A, Nanguanzheng Street#88, Beiling District, Xi'an, 710068 PRC, China
[5] IFREMER, Pointe du Diable, 29280 Plouzané, France

* Corresponding author : Eric Deville, email address : eric.deville@ifpen.fr

Abstract :

Several marine geophysical data and piston-coring surveys acquired during the last decade allow one to better understand the close dynamic interactions between the sand-rich Orinoco turbidite system and the compressional structures of the Barbados prism. These interactions have been active since Eocene time as illustrated by the study of outcrops onshore Barbados Island. Because of strong morphologic and tectonic control in the east-Caribbean active margin, the present-day Orinoco turbiditic pattern system does not exhibit a classic fan geometry. The sea-floor geometry between the slope of the front of the Barbados prism and the slope of the South-American margin induces the convergence of the turbidite channels toward the abyssal plain, at the front of the accretionary prism. Also, whereas in most passive margins the turbidite systems are organized upstream to downstream as canyon, channel-levee and lobes, here, due to the tectonic control, the sedimentary system is organized upstream to downstream as channel-levee, canyons and channelized lobes. Indeed, at the edge of the Orinoco platform, the system has multiple sources with several distributaries and downstream the channel courses are complex with frequent convergences or divergences that are emphasized by the effects of the undulating seafloor tectonic morphologies associated with active thrust tectonics and mud volcanism. On top of the accretionary prism, turbidite sediments are filling transported piggy-back basins whose timing of sedimentation vs. deformation is complex. While erosion processes are almost absent on the highly subsiding Orinoco platform and in the upper part of the turbidite system, they develop mostly between 2000 and 4000 m of water depth, above the compressional structures of the Barbados prism (canyons up to 3 km wide and 300 m deep). In the abyssal plain, the main turbiditic channel develops toward the east and connects with the Vidal mid-Atlantic channel. The sediments transported in this channel are filling several elongated basins linked with fracture zones (notably the Barracuda Basin), and finally end their course in the Puerto-Rico trench, the deepest morphologic depression of the region. Piston-cores have demonstrated that turbidite sediments above the accretionary prism and in the abyssal plain are mostly coarse sandy deposits covered by recent pelagic planktonic-rich sediments, which corresponds to slower sand deposition during the post-glacial sea level rise. Numerical stratigraphic modelling suggests that during the last glacial event, the main depocentres were located above the tectonic prism and in the abyssal plain, at the front of the prism and that, during the Holocene eustatic rise, a large accommodation space formed on the shelf confining sedimentation mostly on the Orinoco deltaic platform and producing a starvation downstream in the turbidite system.

Highlights

► An overview of the nature and architecture of the Orinoco turbidite system is proposed. ► We discuss how the active margin tectonic processes control the turbidite system. ► We discuss the specificity compared with turbidite systems in passive margins. ► Deep-marine erosion processes and sediments transport are described. ► A numerical model is proposed and compared with the actual sedimentary system.

Keywords : turbidite system, active margin, Orinoco, Barbados

INTRODUCTION

Main offshore deltas and deep-sea fans on passive margins (Mississippi, MacKenzie, Amazon, Rio de la Plata, Niger, Nile, Congo, Zambeze, Mahakam, Ob, Yangtse, ...) are characterized by upstream sources of siliciclastic sediments resulting from onshore erosional processes, the location of which is globally more or less constant over long periods of time (several tens of Ma). They are also commonly characterized by deep marine erosion processes at the border of the platform incising the shelf-edge (canyons), by a divergent channel-levees turbidite system along the continental slope (deep-sea fans), and by the deposition of sediments as lobes in the abyssal plain. This classical scheme is not anymore valid in active margin context (Orinoco, Magdalena, Indus, Gange, ...). In this case, the deposition system is controlled by several additional parameters including extensive migration of the main source of siliciclastic input during time, high subsidence rates on the platform, tectonic mobility of the topography of active margins and progressive deformation of sediments within the accretionary prism and sometimes within the abyssal plain ahead of the accretionary prism. Thereby, a major difference between deep sea fan systems of tectonically active margins and their analogues of passive margins is the high versatility of their architecture due to the progressive deformation processes that drastically influences the location of the depocentres, and the nature and geometry of the deposition system. Notably, several points remain poorly understood in turbidite systems deposited on mobile substratum of tectonically active margins, like the global evolution of the sedimentary systems during the migration of the deformations, the sedimentary implications of the dynamic physiography resulting in a system much more complex than a classical fan, and the processes of sedimentation/erosion in the deep sea area incising the tectonic structures. Only few published works describe the deposition systems, the spatial distribution and the geometry of the turbidite reservoirs in tectonically active context. Also, only few explanations have been published about the fact that these tectonically active systems are less prone to develop canyons at the shelf-edge (Orinoco, Magdalena, MacKenzie; Callec et al., 2010; Ercilla et al., 2002). Deep water erosional processes of the tectonic structures are also poorly understood (Mascle et al., 1990; Deville et al., 2003; Huyghe et al., 2004). No specific work have been published concerning the sedimentary and tectonic processes responsible for the progressive incorporation of turbidite sediments inside the accretionary prisms and where should we expect to find good turbiditic reservoir inside the accretionary wedge.

In sand-rich tectonically active systems, previous works have shown punctually that sand rich-deposits can be scattered in piggy-back basins on top of the accretionary prism or in the abyssal plain (Faugères et al., ; Callec et al., 2010) but no available work provides a large scale understanding of the general distribution of sand-rich deposits.

Tectonics and sedimentation processes in a tectonically active area are well illustrated in the zone of interaction between the Orinoco siliciclastic deposition system and the deformation structures associated with the east Caribbean active margin. The Orinoco detrital system develops over a distance of several thousand kilometres, from 3 major South American topographic highs (Guyana Shield in Venezuela, Western Cordillera of Colombia and Merida Andes culminating at Pico Bolivar 4978 m) to the deepest point of the Atlantic Ocean, the Milwaukee deep (-8385 m), in the Puerto Rico Trench (Fig. 1). Onshore, this siliciclastic system develops mostly in the Andean belt and the Caribbean costal belt and their foreland, whereas, offshore, the turbidite system issued from the Orinoco delta is closely tectonically controlled by the deformation processes of both the Barbados accretionary prism and the diffuse plate boundary between North and South America in the Atlantic abyssal plains. Former papers gave local illustrations of some of these processes at the connection between the turbidite system of the Orinoco delta and the Barbados accretionary prism (Biju-Duval et al., 1982; Brown and Westbrook, 1987; Mascle et al., 1990; Faugères et al., 1991; Huyghe et al., 1996, 1999, 2004; Deville et al., 2003; Callec et al., 2010; Patriat et al., 2011; Pichot et al., 2012). The objectives of this paper is to provide a comparison between a fossil system preserved inside the tectonic prism and the active modern system and to provide information of how tectonics controls sedimentation in an active margin and how it controls the incorporation of the sand-rich sediments inside the accretionary wedge. This approach was made in order to provide a better understanding of spatial and temporal variations in geometry and lithofacies organization of reservoir quality sediments in the accretionary complex. For this, we made an integration of partly published data but also unpublished data acquired both offshore and onshore. Finally, stratigraphic modelling is proposed to try to understand better the large scale sedimentary processes.

GEOLOGICAL SETTING

From a geodynamic point of view, the region corresponds to the triple junction area between (1) the North American plate, (2) the South American plate and (3) the Caribbean plate (Fig. 1). It is characterized by complex and multidirectional recent deformations distributed throughout the area. The two American plates are involved into the westward subduction beneath the east Caribbean active margin (Fig. 1). This active subduction is associated with significant seismicity under the volcanic arc of the Lesser Antilles. The seismicity associated with the East Caribbean margin is notably highlighting the geometry of the subduction of the Atlantic oceanic lithosphere beneath the Caribbean plate (Fig. 2). Earthquakes located near the plate boundary are deepening westward to more than 150 km under the volcanic arc of the Lesser Antilles (Fig. 2). North of the active margin, the subduction slab is continuous and extends far to the west below Puerto Rico (Fig. 1). South of the active margin, the seismicity shows that the subduction slab sinks below the island of Trinidad and the Paria Peninsula in north-eastern Venezuela and stops south of the Orinoco Delta Fault Zone (Deville and Mascle, 2012). Earthquakes are expressed in both, the upper plate in the volcanic arc, and also in the subducted slab (Fig. 2). The Barbados accretionary prism, meanwhile, is almost aseismic. The latest GPS studies (Dixon et al. 1998; Demets, 2000; Weber et al., 2000; Jansma et al., 2000; Calais et al., 2002; Mann et al., 2002) showed that the Caribbean plate is moving east-northeast in the direction N70° at a speed of 20 ± 3 mm/a with respect to the North American plate (Fig. 1). Convergence associated with the subduction below the Lesser Antilles volcanic arc caused the deformation of the sedimentary pile and the formation of the Barbados accretionary prism which is one of the largest accretionary wedges in the world (Westbrook, 1975, 1982; Stride et al., 1982; Westbrook et al., 1982, 1983, 1984, 1988; Biju-Duval et al., 1982, 1984; Westbrook and Smith, 1983; Mascle et al., 1988; Mascle and Moore, 1990; Henry et al., 1990; Deville and Mascle, 2012).

In the Atlantic domain, the deformations associated with the relative motion between the North America and South America plates are distributed over a large domain (several hundreds of kilometres from north to south). The rare and diffuse seismicity associated with uncharacteristic bathymetric features is still a source of misunderstanding concerning the exact location of the plate boundary between South America and North America. However, the kinematic models have demonstrated quite early the existence of this border (Minster and Jordan, 1978; Roest and Collette, 1986; Klitgord and Schouten, 1986; Smith and Mueller, 1993; Campan, 1995; Gordon, 1998). These deformations are well expressed in the area between the Fifteen-Twenty transform fracture zone to the north and the Marathon fracture zone to the South (Roest and Collette, 1986; Roest, 1987; Sumner and Westbrook, 2001; Pichot et al., 2012; Fig. 1). In this wide deformation zone, the oceanic lithosphere is characterized by a system of transform fracture zones partly recently re-activated and locally associated with recent folds trending WNW-ESE. We observe in particular, in this area, different sea floor highs associated with the relative movements between North and South America, the most noticeable being the Barracuda ridge, the Tiburon rise and the Researcher ridge (Birch, 1970; Brown and Westbrook, 1987, Mueller and Smith, 1993; Patriat et al., 2011; Pichot et al., 2012; Fig. 1).

Marine geophysical data (multibeam and seismic lines), such as data acquired in 2007 during the Antiplac survey, in the North-South Americas-Caribbean triple point (Barracuda and Tiburon ridges area) showed that the deformation of the plate boundary between the north and south American plates affects several structures located in the abyssal plain, in front of the Barbados accretionary prism (Patriat et al., 2011; Pichot et al., 2012). Notably, the Barracuda ridge and Tiburon rise are natural barriers which have been tectonically reactivated (faulting, folding, uplift and/or tilting) recently during Pleistocene times (Patriat et al., 2011). This recent deformation has generated relieves up to 2 km high with associated erosion processes localised notably along the northern flank the Barracuda ridge (Pichot et al., 2012). In this area, the main depressions and fracture zones are filled with Pleistocene turbidite sediments, as in the Barracuda trough, north of Barracuda ridge which is characterized by an elongated E-W zone of low gravimetric values (Fig. 3). The subduction of these ridges induces deformation processes within the Barbados accretionary prism. These asperities within the Atlantic oceanic lithosphere are correlated with zones of intense seismic activity below the volcanic arc (Bouysse et al., 1990; Ruiz et al., in press).

In the studied area, the opening of the central Atlantic Ocean separating the American and African plates began in the Late Jurassic. The oldest portions of the oceanic crust (Upper Jurassic to Lower Cretaceous) were subducted beneath the Caribbean plate. Portions of this crust are now obducted in Colombia, Venezuela and Greater Antilles (Mattson and Pessagno, 1979; Dupuis, 1999, Baumgardner et al., 2008). Jurassic-Lower Cretaceous oceanic crust is also present in the Demerara abyssal plain in front of the Barbados accretionary prism, along the margin of South America west of the Demerara Plateau (Westbrook, 1984; Deville and Mascle, 2012). Indeed, the East Caribbean active margin has progressively migrated toward the east with respect to the central Atlantic probably since Cretaceous times (Pindel et al., 2006). During this several hundreds of kilometres long displacement, the sediments deposited on top of the Atlantic oceanic lithosphere (including turbidites brought by the paleo-Orinoco) have been progressively incorporated in the core of the Barbados accretionary prism which corresponds to the leading edge of the east Caribbean active margin. Indeed, the Orinoco drainage basin has largely contributed to turbidite sedimentation in the Demerara abyssal plain since at least Eocene times (Wright, 1984; Beck et al., 1990; Di Crocce et al., 1999;

Figs. 4, 5, 6, 7). The detritic material was provided by erosional processes mostly from the Andes but also largely from the Guyana shield (Schmitz et al., 2002). Before Late Miocene times, the Paleo-Orinoco drainage basin included parts of the present-day drainage basin of the Amazon River until Late Miocene when sediments were finally transported toward the Amazon mouth only since Miocene times. But the Orinoco drainage basin has also drastically changed during Tertiary times and during this period the Orinoco delta has migrated eastward over more than 500 km because of the eastward deformation in north Venezuela due to the Caribbean plate / South America relative movements (Beck et al., 1990; Pindell, 2006). The foreland of the accretionary prism is affected deformations processes associated with the relative displacement between the South American and North American plates. Also, the Orinoco turbidite deposits partly cover the Barbados accretionary prism in its southern part. In this area, close to the Trinidad-Venezuelan continental platform, the seafloor is regular and punctually disturbed by isolated mud volcanoes (Brami et al., 2000; Rutledge and Leonard, 2001; Deville et al., 2003; Deville et al., 2004; Moscardelli et al., 2006; Deville et al., 2006; Deville and Mascle, 2012). Downslope, the geometry of the seafloor of the southern Barbados area, which controls the channel courses, is controlled by tectonics and mud volcanism processes generating local highs and syntectonic piggyback basins (Biju-Duval et al., 1982; Mascle et al., 1990; Gonthier et al., 1994; Huyghe et al., 1996, 1999, 2004; Callec et al., 2010; Faugères et al., 1993; Griboulard et al., 1991, 1996). The seafloor bathymetry in the successive piggyback shows clearly a step geometry each of these basins showing an average characteristic seafloor depth (see piggyback basins 1 to 5 in Fig. 9). In some areas, the development of ramp anticlines has formed closed basins disconnected from the turbidite sources. As a consequence, these starved basins show relatively deep bathymetry compared to the surrounding basins (Figs 8, 9). Finally, the Orinoco turbidite develops very far in the Atlantic abyssal plains in between the relieves associated with the deformation processes between the South American and North American plates.

ANCIENT TURBIDITE MATERIAL ACCRETED WITHIN THE ACCRETIONARY PRISM

Background

As mentioned above, the Barbados accretionary prism being active since at least Eocene times, it incorporated ancient deep turbidite material. A good understanding of these fossil turbidite systems is crucial in terms of hydrocarbon exploration because they are prone to correspond to good reservoir, as well-illustrated by the oil which is produced since decades in these types of Eocene deposits in the Woodbourne field, offshore Barbados Island (Hill and Schenk, 2005). The characteristics of turbidite deposits which are deformed within the Barbados accretionary prism are well-evidenced onshore Barbados Island, notably along the outcrops of the crest of Chalky Mount (Senn, 1940; Larue and Speed, 1983, 1984; Larue and Provine, 1988; Biju-Duval et al., 1985; Deville and Mascle, 2012; figs. 5, 6). This crest offers a very nice example showing the nature and architecture of deep sandy turbidites of Eocene age (Ypresian-Lutetian, Scotland Group) corresponding to the ancient turbidite system incorporated within the Barbados accretionary prism. These sediments can be compared with the Eocene turbidites found at the front of the Barbados accretionary prism in ODP site 674 and in the abyssal plain in ODP site 672 (Mascle and Moore, 1990; Fig. 1, 3). In Barbados, these turbidite sandstones are stratigraphically covered by Late Eocene-Oligocene pelagic carbonates, locally by Miocene sandstone and carbonate, and finally by the Quaternary coral reef (Senn, 1940; Saunders et al., 1984; Deville and Mascle, 2012).In this section, we present briefly the characteristics of these outcrops (reservoir architecture, depositional model, reservoir quality) as a reference of the ancient turbidite material accreted within the core of the prism in order to compare it with the present-day turbidite system which is presenter later. The previous works of Pudsey and Reading (1982), Larue and Speed (1983), Biju-Duval et al. (1985), Kasper and Larue (1986) and Larue and Provine (1988) showed that the depositional environment of this formation corresponded to a deep turbidite system sourced from the South American continent. These deposits are assumed to have been deposited below the Carbonate Compensation Depth (CCD; Larue and Speed, 1983), which partly explains their low carbonate content (mostly < 2 %; Fig. 7), their low content in pelagic fossils and their low amount of cementation. Some sandstone units reach several tens of metres thick, with porosities up to 40% (Speed et al., 1991). We studied turbidite sequences about 90 m thick and one kilometre-long which have been verticalized by compressional tectonics inside the Barbados accretionary prism. Six detailed sedimentological sections were studied in details to identify and characterize the geometry of the sedimentary bodies, and to provide information about the deposition context (Figs. 5, 6).

Description

In these outcrops, we distinguished three main units (A, B, C). Unit A (uppermost visible part) and unit B (Fig. 6) are mainly characterized by amalgamated turbidites. The two intervals are separated by a continuous heterolithic level associated with the blanketing of unit A. The lower unit (A) is less than 12 metres thick and only the last few metres are visible at the outcrop. This unit is mainly composed from bottom to top of the following facies associations: slurry, amalgamated turbidites and heterolithic deposits. The later represent amalgamated turbidites at the top of the unit A. The intermediate unit (B) has a thickness of about 55 metres. The deposition of this unit is dominated by a succession of amalgamated turbidites that are locally several tens of centimetres to tens of metres thick. Laterally, these levels pass from massive to thinner facies and heterolithics, either gradually (lateral change of facies) or by sharp contact (overbank deposits). The upper unit (C) has a thickness of about 25 metres and only its base is visible at the outcrops (Fig. 6). It comprises three facies (1) coarse-grained, trough cross-bedded sandstone), (2) finer-grained sandstone showing ripples and (3) mainly heterolithics and shale).

Among the outcrops of Chalky Mount, amalgamated turbidites of Unit B have the best reservoir potential. Indeed, they display a good lateral continuity, due to the high connectivity of the sedimentary bodies). The internal heterogeneities correspond to discontinuous heterolithic or shaly deposit levels, with a maximum thickness of 1 metre. The unit C includes channelized turbidites which are the best potential reservoir of this unit whereas in this unit C, heterolithic levels (levee deposits and overflow) may represent important permeability barriers.

The organic matter which is mostly present in the F9 terms (Fig. 5) of the turbidite sequences (TOC < 1.5%; S2 < 1.5 mg HC/ g rock) is immature (T_{max} < 435°C) and is purely of type III and corresponds to detrital organic matter (plant fragments; OI < 40 mg CO_2/g rock; Fig. 7).

Interpretation

The sedimentary facies associations observed in the outcrops of Chalky Mount correspond to high and low density gravity deposits in a deep water environment (Mutti, 1992). The adopted facies classification (Fig. 5) is based on the concept of the transformation of a gravity flow during its displacement, which evolves from laminar and cohesive to hyper-concentrated, and then to high density turbulent flows. The continued incorporation of water downslope due to turbulence and the deposition of the coarser fraction leads to further dilution of turbidity flow, which becomes low in density.

Sediments show a vertical organization related with hydrodynamic flow transformation of turbidity currents from cohesive flows (F1, F2) to high density (F4 to F8) and density (F9) turbulent flows. Here, the full facies succession as described by Mutti (1992), modified by Garcia et al. (2004) and Joseph et al. (2012) was not observed. Notably, terms between F1 and F3 (debris flows and hyperconcentrated flows) were not observed.

We interpret the top of unit A as a phase of abandonment of the filling and the amalgamated turbidites of Unit B as a deep-marine braided channels. The three facies associations of unit C are probably genetically related: channel-fill turbidite deposits (coarse-grained, trough cross-bedded sandstone), levee deposits (finer-grained sandstone showing ripples) and overbank deposits (mainly heterolithics and shale). This unit C is interpreted as channelized turbidites corresponding to the filling of a main transit channel.

The lateral connectivity of the sand bodies of unit B is expected to be high due to the high sand content. Few shale breaks exist which may however impact the average vertical connectivity of the amalgamated turbiditic units. The potential reservoir connectivity is high within the channelized turbiditic units of Unit C. Between the channels, levees and overbank deposits are associated with heterolithic deposits which may affect the vertical connectivity of the main channelized turbiditic units.

From their overall characteristics (nature and architecture), the turbidite sandstones outcropping at the Chalky Mount crest onshore Barbados can be regarded as the middle part of a deep-marine sand-rich turbidite system and they are believed to be similar to the modern turbidite sediments deposited in the abyssal plain at the tectonically active front of the Barbados accretionary prism.

THE MODERN TURBIDITE SYSTEM

The upstream feeding system

The turbidite system issued from the present-day Orinoco delta develops at the eastern edge of the East Caribbean active margin partly above the large southern part of the Barbados accretionary prism and downslope at the front of this prism, within the Demerara abyssal plain (Biju-Duval et al., 1982, Brown and Westbrook, 1987; Mascle et al., 1990; Faugères et al., 1991, 1993; Deville et al., 2003; Callec et al., 2010; Deville and Mascle, 2012; Fig.1). Syntectonic turbidite sedimentation in the southern area of the Barbados accretionary prism and in the deep Demerara plain contributes to the growth of the Barbados accretionary prism, by piggyback basin development above the prism and by frontal accretion at the convergent front (Mascle et al., 1990; Huyghe et al., 1999; Callec et al., 2010). The turbidite sediments which are deposited on top of the Barbados accretionary prism and in the Demerara abyssal plain at the front of the Barbados accretionary prism originate mainly from erosional processes of the south American continental crust, mostly from the Andes, but also from the Caribbean coastal ranges and the Guyana shield. The source of siliciclastic sediments being issued from South America, the Barbados prism is thinning northward. In the shelfal area south and east of Trinidad, the recent deformation is mainly characterized by both strike-slip and normal faulting which have favoured the development of large accommodation areas for recent sediments in the Columbus Basin, southeast of Trinidad and in the Orinoco platform ("plataforma deltana") in the offshore Venezuela (Galbraith and Brown, 1999; Gersztenkorn et al., 1999; Heppard et al., 1998; Wood, 2000; Gibson and Bentham, 2003; Moscadelli et al., 2006, 2012).

As it was probably the case during earlier highstand period, sediments found today in the Orinoco turbidite system are brought by the Orinoco River, plus a far contribution coming from the Amazon River and the river system of the Guyana margin (Herrera et al., 1981; Meade, 1990; Warne et al., 2002; Aslan et al., 2003). Indeed, significant siliciclastic material (clays, silt and fine sand) issued from the rivers of the Guyana margin and from the Amazon is transported north-westward by the Guyana Littoral Current (GLC) along the south American shore line (Warne et al., 2002; Alfonso et al., 2006; Anthony et al., 2010; Fig. 1). The transport efficiency of the GLC is due to its high velocity (Metcali, 1968; Herrera et al., 1981; Curtin, 1986) reaching locally up to 1 m/s, the mean speed being 0.4 m/s (Bulgakov et al., 1998; Warne et al., 2002). This current induces the development of mud banks close to the shore (Anthony et al., 2010) and offshore sand bars close to the shelf edge (Van Andel, 1967; Alfonso et al., 2006). Part of the flow may however be diverted to the continental slope, inducing a dense network of gullies such as east of French Guyana, or inducing fields of sedimentary waves as offshore Surinam and Guyana (Ercilla et al., 1998).

Compared with the Amazon system where mostly fine material is delivered to the sea (clay-rich system), the Orinoco River has built a delta from bed loads (quartz arenite), suspended loads, clay and organic matter (see later) and a small amount of shallow marine shell debris.

From today's Orinoco drainage area which is close to 10^6 km^2, the annual water flux delivered to the sea varies between 1050 m^3/s and 82100 m^3/s depending on the season, the mean flux being around 35000 m^3/s, *i.e.* 1.1 x 10^{12} m^3/a (Warne et al., 2002). The suspended sediments carried by the modern Orinoco river is about 150 10^6 ton/a (Meade, 1994) including about 20% of sand. On the other hand, the Amazon drainage basin being a very wide drainage area (about 6 10^6 km^2) and the annual water flow at the Amazon mouth is very high (6.3 x 10^{12} m^3/a). It is the largest water discharge to the World Ocean. The modern suspended sediment discharge of the Amazon is high, about 1200 x 10^6 ton/a, that makes it the second largest discharge to the World Ocean with a maximum input occurring in March-April (4–6 x 10^6 tons/day). The solid sediment discharge is much less rich in sand (5–10%) compared with the Orinoco. From the total sediment discharge of the Amazon, 15–20 % are advected to the Guyana shelf and about 60 10^6 tons/a are deposited on the Orinoco shelf (Warne et al., 2002). So, in the present-day highstand period, the solid sedimentary flux issued from both the Orinoco and the Guyana Coastal Current on the Orinoco platform is estimated to be close to 210 x 10^6 ton/a taking into account the several published data (Van Andel, 1967; Milliman *et al.*, 1982; Rodriguez and Meade, 1983; Meade, 1990; José-Mendez, 2000; Warne et al., 2002).

During the past lowstand periods the framework of this feeding system was probably very different because the Guyana-Orinoco platform was partly emerged or very shallow and the sediments were then very probably directly transported to the shelf-edge, without storage on the shelf. It is during these lowstands periods that the sand-rich turbidite system of the Orinoco, the mud-rich deep water cone of the Amazon and the secondary systems of the Guyana margin (Veeken, 1983; Loncke et al., 2009) have been mostly fed by siliciclastic material transported by the rivers directly to the slope (Flood et al., 1997; Normak et al., 1998; Jegou et al., 2008; Faugères et al., 1991; Callec et al., 2010).

Channel pattern on top of the accretionary prism

As mentioned in introduction, due to its location within an active margin, the offshore Orinoco turbidite system is not a passive margin delta-fed deep-sea fan. The transport and depositional system are controlled by the compressional structures and mud volcanism processes within the Barbados accretionary prism, as well as the deformation processes of the ocean lithosphere in the Demerara abyssal plain. Notably one obvious consequence is that this turbidite system does not exhibit a classic fan geometry. The bathymetric confinement between the Barbados accretionary prism and the continental slope of the Guyana margin forces the turbidite channels to converge toward the abyssal plain, at the front of the accretionary prism (Fig. 1).

The evolution of the channel architecture of the recent Orinoco turbidite system on top of the Barbados accretionary prism from the upper slope to the abyssal plain has partly been described in former publications (Huyghe et al., 2004; Callec et al., 2010). In the upper slope (above 1500 m of water depth), the system has multiple sources with several distributaries. Downslope (between 1500 m and the front of the accretionary prism), the channel courses are more complex showing irregular sinuosity and frequent convergences or divergences, which are emphasized by the morphology of the seafloor. In several locations, avulsion processes are due to migration of the channel course related to the progressive deformation of the seafloor (Callec et al., 2010).

This area is also characterized by superficial flows issued from mud volcanoes and when high sedimentation rates interfere with mud volcanism processes, it is common to observe the stacking of mud volcano edifices progressively covered by turbidite sediments (Deville et al., 2006; Fig. 9). Also, commonly, gravity mass-flows are sliding on topographic slopes in the piggyback basins (*in-situ* sources), the most massive of these mass-flows being well evidenced on the seismic data (Chennouf, 1987; Faugères et al., 1993; Deville et al., 2006; Callec et al., 2010; Fig. 8, 9).

Channels which formed in the piggyback basins above the accretionary prism are characterized by well-developed aggrading channel-levee complexes with highly sinuous and meandering geometries (Fig. 8). The channels are filling these syntectonic piggyback basins of the prism, and in some locations, they their levees are covering early deformation (fold and thrust structures; Callec et al., 2010; Fig. 9). The general course of the channels is controlled by the orientation of the elongated piggyback basins. Severe inflections of their course toward the east or the southeast are observed when they incise the NE-SW trending ramp anticlines of the tectonic prism, notably in the frontal part of the accretionary wedge (Fig. 8). In the frontal zone of the tectonic prism, channel courses are largely controlled by the complex morphology of the seafloor and their geometries evolve systematically to deep incisions (canyons). Therefore four recent canyons with several terraces deeply incise the frontal anticlines related to active thrusting. It is noticeable that these canyons, even the more erosive ones, have clear meandering courses which might predate the folding process (Fig. 8).

Long distance channel pattern in the abyssal plain

In front of the tectonic wedge, V shape erosional channels with several terraces characterize the transition zone toward the abyssal plain. Northward, minor channels run along the front of the accretionary prism (Callec et al., 2010; Fig. 8). In the abyssal plain, distributary channels have developed (Belderson et al., 1984; Ercilla et al., 1998; Callec et al., 2010) with a main low-sinuosity channel, which presents a broad geometry with low-relief aggrading channel-levee architecture. In this area sandy distal lobes are observed with plane-convex elementary bodies, which are characteristic of sandy turbidite lobes (Callec et al., 2010). At 12°N, east of the tectonic front of the Barbados accretionary, the main turbidite channel extends largely eastward away from the front of the Barbados prism for more than 500 km (Ercilla et al., 1998) and joins the Vidal Mid-Ocean Channel (Embley et al., 1970; Embley and Langseth, 1977; Baraza et al., 1997, 2000; Figs. 1, 4). As such, the Orinoco distal turbidite system is indeed connected with the Vidal channel which is trending northward and joins the eastern part of the deep Barracuda trench, north of the Barrucada ridge (Figs. 1, 4, 10). In the Barracuda trough, we know for a long time that a modern sand-rich channel system exits carrying coarse material and which is not sourced by the closest emerged land (Antilles Islands) but instead the channel system is running from east to west, from the Atlantic toward the Antilles (Birch, 1970). These sediments are sourced from the East by the Orinoco turbidite distal system, through channels transiting in the Demerara abyssal plain, which is consistent with the fact that the flat seafloor of the Barracuda trough is gently deeping westward (Pichot et al., 2012), the average dip value being very low (0.0175°). The thickness of the recent Quaternary sediments filling the Barracuda trough is very high (locally higher than 2 sTWT, corresponding probably to more than 2 km; Patriat et al., 2011; Pichot et al., 2012; Fig. 11), which is consistent with the data collected at DSDP drilling site 27 (Bader et al., 1970) and ODP site 110 (Mascle and Moore, 1990). These Quaternary sediments in the Barracuda trough show locally spectacular evidences of very recent (at least Quaternary) to active deformation in the pre-existing fifteen-Twenty transform fault system. The channel system occurring in the Barracuda trough is then flowing in between the deep sea relief of the western part of the Barracuda trough (Figs. 12, 13), toward the Puerto Rico trench (Tucholke, 2002; Brink et al., 2004). This depression, the deepest in the Atlantic domain (Fig. 1, 4) finally captures all the remaining sediments of this turbiditic system after their very long sedimentary transit system (more than 3000 km long) running from the shore of south America to the north of Puerto Rico.

FACIES DISTRIBUTION

Turbidite sedimentation on top of the accretionary prism

We have seen above that the channel pattern is different from passive margin delta-fed deep-sea fans but the Orinoco turbidite system shows also some particularities regarding the spatial distribution of the sedimentary facies. The different facies that have been distinguished in the study area on top of the accretionary prism south of 13°N are shown on the map of the Figure 8. This mapping results from the compilation of piston cores in this area and from the interpretation of multibeam data (EM12 bathymetric and backscattering), seismic data and 3.5 kHz profiles. Coring results have been partly published by Faugères et al. (1991, 1993), Gonthier et al. (1994), Deville et al. (2006) and Callec et al. (2010). These data display the spectacular complexity and diversity of facies distribution compared with turbidite systems in passive margin context, notably on top of the accretionary prism (Fig. 8). From upstream to downstream, the following general tendencies are observed. Starting from the platform, fine-grained sandy deposits are stored on the outer shelf (Van Andel, 1967; Alfonso et al., 2006). In the slope close to the shelf edge, the channels are currently overlapped by recent deposits, mostly mass-flows from the upper continental slope (Brami et al., 2000; Moscardelli et al., 2006; Callec et al., 2010; Fig. 8). As such, the trace of the channels in the upper slope tends to be covered by these very recent sediments (Fig. 8).

Cores collected in this upslope area show mostly thin hemipelagic sedimentation with some silty intercalations and very thin turbidites. Cores taken downslope, in the area where the channel system is well expressed at the sea bottom, have found levee deposits corresponding to thin and fine-grained turbidites made up of centimetric laminations (parallel or rippled) of silt and fine sands. These deposits developed on the sides of the channels but they are also found on top of massive uplift structures (Deville et al., 2006). These cores taken on the sides of the turbidite channels on top of the accretionary prism show episodic or continuous successions of thin-bedded sandy turbidites with Bouma-type sequences characterized by terms Tb, Tbc, Tce, Tde (Fig. 5B). Figure 14 illustrates an example of core collected in a levee of one the main channels, with a gamma-ray and magnetic susceptibility characterization and X-Ray radiography. Gamma-ray attenuation is very constant, showing the homogeneity of the fine turbidite material. The magnetic susceptibility anomalies are directly related to the occurrence of micro-pyrite associated with the main organic-rich levels. X-ray radiography reveals the very fine character of the turbiditite sequences. The upper part of the core shows a progressive increase in calcium carbonate. In all the cores collected on top the Barbados prism, the organic matter shows typical terrestrial type 3 characteristics corresponding to transported detrital plant fragments (Fig. 7). Locally, gravity mass-flows also occurred (Callec et al., 2010) reflecting slope destabilization processes and significant detrital flux associated with proximity of the detrital sources from the Orinoco platform. The topographic highs on top of the folds of the accretionary prism are characterized by homogeneous hemipelagic sedimentation (Callec et al., 2010). As coring attend made in the deep incision were not successful, the piston core being folded because of highly compacted sediments in these areas, it was only possible to recover cores from the channel axis, when heterolithic mass flows are present inside the canyons (Callec et al., 2010). In the closed (starved) piggyback basins above the accretionary prism which are disconnected from the present–day turbidite channels, thin sandy turbidites have also been found. They correspond probably to ancient turbidite channels which are now abandoned (Callec et al., 2010). More generally, we interpret the cores taken on the sides of the turbidite channels on top of the accretionary prism as related to low density turbulent flows whereas the final blanketing of carbonate deposits would correspond to an evolution toward hemipelagic conditions which is a constant feature in all the cores collected in this area (Callec et al., 2010).

Turbidite sedimentation in the abyssal plain

In the whole studied area of the Demerara abyssal plain, the data are not sufficient (in quality and quantity) to propose a detailed mapping such as the one shown in Figure 8 on the accretionary prism. Notably, the areas north of 13°N being in deep water, the 3.5 kHz data are of very poor quality and only some coring results are available. Nevertheless, all the available coring surveys have shown that turbidite sediments deposited in the abyssal plain at the front of the accretionary prism are mostly sand-rich deposits (Faugères et al., 1991; Callec et al., 2010). The occurrence of sandy layer have even been found in very distal parts like in the Barracuda trough where locally sand-rich turbidites interbedded with organic-rich layers since long have been described (Birch, 1970). The sand-rich sediments at the front of the accretionary prism correspond to massive sandy turbidites characterized by sand-clay mixing intervals (slurry beds) reflecting erosion processes of the seafloor. Some characteristic cores are shown in figures 15 and 16, with gamma-ray, magnetic susceptibility and calcium carbonate characterization and an example of X-Ray radiography in Figure 15. In the abyssal plain, at the canyon exit immediately east of the Barbados thrust front, the levee deposits correspond to fine to medium sandy turbidites with intercalation of organic-rich material (Fig. 15). Gamma-ray attenuation shows notably the relative poorness in massive clay-rich intercalations and the magnetic susceptibility anomalies are mostly associated with organic-rich intercalations and pyrite occurrence. The X-ray radiography of these cores outlines clearly an internal structure made of fine-medium turbidites (parallel to rippled). Downstream, away from the front of the accretionary prism, all the recovered cores in the abyssal plain were made of massive coarse sandy turbidites with organic-rich intercalations (Fig. 16). The thinnest levels characterized by low gamma-ray values and high magnetic susceptibility might correspond to ash-rich layers. Here again, the organic matter (TOC < 2%; S2 < 2 mg HC/g rock) present in the abyssal plain turbidites is purely of type 3 and corresponds to transported plant fragments (OI < 200 mg CO_2/g rock; Fig. 7). The carbonate content of these turbidite sediments is generally low (< 10%).

Periods of activity of the turbidite system

The period of main activity of the modern turbidite system which is recorded in the sediments collected by piston cores (< 10 m deep) corresponds probably to the last lowstand of sea level which corresponds to the last glacial event. This interpretation is compatible with dating with ^{14}C methods of an organic-rich horizon interbedded within turbidite layers in the CARAM 17 core at a depth of 4.68 m gave an age of 24480 $\pm$ 140 BP (Fig. 14), so during the latest Pleistocene glacial event (Visconsin/Würm). Since that period of main turbidite activity, the turbidite system became less active or even locally inactive in the deep water area. Indeed, we found evidences of active turbidite sedimentation only close to the shelf edge. The relative absence or thinness of the turbidite draping in channels further downslope supports low sedimentation rates in the turbidite channel system related to the rise of sea level since the last glacial lowstand. The sand-rich turbidite sediments deposited in the Barbados accretionary prism area and in the abyssal plain are indeed systematically covered by a few tens of centimetres of recent pelagic planktonic-rich sedimentation which indicates that sand deposition has decreased or stopped since the last ice age (Figs. 14, 15, 16). These foram-rich uppermost oozes are much richer in calcium carbonate than the turbidite below (Figs. 14, 15, 16). The contrasted periods of activity of the turbidite system which have been demonstrated since the last glacial period suggests cyclic activity with high rates of turbidite sedimentation during lowstands and moderate activity during highstands.

DEEP WATER EROSION PROCESSES

Slope instabilities and induced mass-flows are common in the accretionary prism notably at the frontal parts of ramp anticlines where steep slopes can develop (Chennouf, 1987; Faugères et al., 1993; Padron de Carillo, 2008; Callec et al., 2010; Fig. 8). Moreover, erosion processes directly related with turbidite processes are widespread in the Orinoco system. Despite of a very common feature of global distribution of large submarine canyons (Harris and Whiteway, 2011), the peculiarity of the Orinoco deposition system is that no significant recent incision developed on the Guyana-Orinoco shelf break. This is confirmed by intensive oil and gas exploration in the offshore Trinidad and in the Orinoco platform (‘plataforma deltana’) in the offshore of eastern Venezuela (Erlich, 1992; Di Crocce et al., 1999; Wood, 2000; Brami et al., 2000; Moscardelli et al., 2006; 2012; Moscardelli and Wood, 2007). There is also no significant erosion along the upper part of the turbiditic system, in the upper slope, as already noticed by Mascle et al. (1990), Brami et al. (2000), and Callec et al. (2010). Erosion occurred mostly in deep-water (between 2000 and 4000 m of water depth) where it affects largely the fault-bend folds of the Barbados accretionary prism (Mascle et al., 1990; Deville et al., 2003; Huyghe et al., 2004; Callec et al., 2010; Fig. 8, 17). In the erosional area, ramp anticlines and abundant sedimentary mobilization (mud volcanoes) directly control the channel courses by diverting and confining the turbidite flows. Incised channels show irregular meandering sinuous courses in the flattest areas. Where channels cut high-relief structures, they are more confined without levee or with asymmetrical levees and they show deep incisions with a characteristic U shape (Fig. 8). Downslope, at the tectonic front of the Barbados accretionary prism channel courses evolve systematically to canyons with a progressively increasing depth of incision. In the thrust front zone, meandering canyons directly cut the frontal anticlines of the Barbados accretionary prism (Figs. 8, 17).

Larger canyons show a maximum of 3 km width and 300 m depth. Mean dips of slope of canyon walls are steep, locally higher than 15°. In the frontal folds of the accretionary prism, the channel course was probably pre-existing before the development of the final structure of the folds (syntectonic erosion). Immediately east of the tectonic front, the main channel presents also canyon geometry with asymmetric levee deposits and several internal terraces appear in both flanks of the main channel. The occurrence of shifted terraces in both flanks highlight obviously that erosion occurred in different phases of successive incisions leading to the development of several terraces probably due to the superposition of two mechanisms: the tectonic activity of the deformation front characterized by progressive tectonic uplift and the superimposition of the fluctuations of the Orinoco turbidite system activity (see above). Probably, successive erosion steps occurred during cyclic phases of relative lowstand of sea level when the transit of the sand-rich turbidites towards the abyssal plain was the strongest.

During these relative lowstand events there was a sediment bypass with transit of sand-rich coarse-grained sandy sediments responsible for the erosion in the canyons.

Erosion is also found in deep water, very far away from the tectonic front of the Barbados accretionary prism in several locations of the turbidite system. Nice illustrations are shown notably in Baraza et al. (2000) in the Vidal Mid-Ocean Channel. Incisions are found also notably at the transition between the Barracuda trench and the Puerto Rico trench (Fig. 13).

TECTONO-SEDIMENTARY PROCESSES AT THE TECTONIC FRONT

Frontal accretion processes of the sand-rich deposits in the abyssal plain

As seen above, numerous interactions between tectonics and sedimentation occur in the prism (tectonic control on channel course et erosion processes, sedimentary tilting, slope destabilization, ...). Moreover, at the tectonic front of the accretionary prism specific processes occur. Indeed, this tectonic front has progressively migrated toward the abyssal plain through time in relation with the convergence between the Caribbean plate and the American Plates. This process being associated with frontal accretion processes, the sand-rich turbidite deposited in the abyssal plain (channel-levee system and sandy lobes deposits) have been gradually incorporated into the core of the accretionary prism whereas contemporaneous sediments deposited on top of the frontal folds of the tectonic prism correspond to thinner hemipelagic sediments (Fig. 18). As a consequence, the sand-rich levels would be found progressively deeper into the stratigraphic pile toward the core of the prism (Fig. 18). Once accreted in the tectonic prism these levels should then provide good reservoirs with good lateral continuity which are covered by hemipelagic sediments.

Slope destabilizations

As mentioned above, kilometres-long mass-flows are common along the tectonic front of the Barbados accretionary prism, some being mapped on figure 8. Aside of these local mass-flows, between 12 and 14°N, the tectonic front of the Barbados prism is largely affected by spectacular slope destabilization processes over a much wider area (Figs. 8, 19). This is well characterized on bathymetric data by a very chaotic topography which can be interpreted as a zone of gigantic mass-flows. This very wide phenomenon that destabilised the whole slope of the tectonic front in this area might be related with the destabilisation of gas hydrates which has necessarily occurred during the rise associated with the tectonic thickening of the Barbados prism. Indeed, this area is since long known as an area where bottom simulating reflectors (BSR) characterizing the occurrence of gas hydrate are widely developed (Fergusson et al., 1993; Deville et al., 2003). The simple tectonic uplift of the sea bottom related to the tectonic activity of the front of the prism is susceptible to have reduced the thickness of the stability zone of the gas hydrate inducing sudden massive free gas release in the sediments at the base of the gas-hydrates stability zone triggering massive slope instability.

NUMERICAL MODELLING APPROACH

Objectives

For a better understanding of the interactions between tectonic and sedimentation processes and notably the channel pattern and facies distribution of the sediments in relation with the tectonic features of the area, a 3D-numerical stratigraphic modelling of the modern Orinoco turbidite system was performed using Dionisos (Granjeon and Joseph, 1999). This 3D stratigraphic model quantifies the geometry and the nature of sedimentary strata by coupling transport equations and mass conservation principle. Three main physical processes are taken into account ateach step of evolution : creation of accommodation space (eustasy, subsidence, compaction ...), sediment supply (basement and sediment erosion, carbonate production, fluvial supply ...) and sediment transport.

Detailed fluid dynamics are not calculated in Dionisos as its goal is to simulate the large-scale evolution of sedimentary basin. All sedimentary processes leading to the transport of sediment are lumped in two large-scale processes: a slow hillslope creeping and a fast water-driven transport, both rule by a diffusion law:

$Q_s = (K_c + K_w \, q_w^n) \, S$

with $q_w = Q_w/Q_{wo}$

where Q_s is the flux of sediment $[L^2T^{-1}]$, K_c is the creeping diffusion coefficient $[L^2T^{-1}]$, K_w is the water-driven diffusion coefficient, q_w is the dimensionless water flux [-], and S the local topographic slope [-]. Q_w is the actual water flux $[L^2T^{-1}]$ and Q_{wo} the reference water discharge, equal to 0.1 m^2/s. Typical values for the transport parameters are K_c = 0.01 to 0.1 km^2/ky, K_w=100 to 1000 km^2/ky, and n=1.2 to 1.7

The creeping of sediment is assumed to be proportional to the local slope of the landscape, leading to a linear sediment transport ($Q_s=K_c$ S). As Dionisos is mainly working from fluvial plain to deep-sea environments, it is assumed that depositional slopes are gentle (i.e. less than a few degrees) and that hillslope creeping can be simulated using a simple linear diffusion equation ($Q_s=K_w\ q_w^n$ S).

The faster and most important process is the water-driven transport. At a geological time scale, one usually assumed that the upscaling of local-scale transport processes leads to a large-scale fluvial transport equation, which can be written in the form of a diffusion equation. Once again, this diffusion law is not valid to reproduce the detailed dynamics of water and sediment flows ; on the contrary, this empirical law has been used in various forms to study the large-scale and long-term evolution of scarps, alluvial fans, fluvial systems, deltas and continental margins. Recent studies based on flume experiments demonstrated that this law could be used to simulate the time-averaged fluvial transport of sediment (Paola et al., 1992; Postma et al., 2008), although pointing out that insufficient data are available to verify the value of the diffusion law for real-world prototypes (Postma & Van den Berg van Saparoea, 2007). In our model, it is assumed that, at a source-to-sink scale and over long time span (greater than a few thousands of years), sediment transport can be simulated using this nonlinear water-driven diffusion equation. In our deep-marine study, the use of the diffusion law implies that turbidity currents are mainly river-fed hyperpycnal flows, and that the action of deep-marine currents are negligible faced to the strength of these hyperpycnal flows.

The key parameter that rules this water-driven sediment transport is the water flow. In our Dionisos model, a multiple-direction method is used to route the water flow across the simulated area. All water coming into a cell is distributed to all its local lower neighbours, according to the slope ratio. This multiple-direction method better handles diverging flow than other classical water flow routing algorithms (such as the single-direction methods), and is well adapted to simulate overland sheet flow, braided systems and large-scale alluvial fans and turbiditic systems.

Parameters used for the modelling

The area covered by the modelling is shown in Figure 20. The simplified grid used for the modelling is 1200 x 1200 km wide, with 10 x 10 km elements (Fig. 20). It includes the whole

Orinoco turbidite system, as well as the Barbados accretionary prism and the abyssal plain at the front of the Barbados prism. The objectives of this model being to understand the general features of the modern turbidite system, we made the simulation only for the last 50 ka and because of this we neglected the topographic changes during this relatively short period of time (lateral tectonic displacement during this period of time being less than 1 km, whereas the grid used in the model is 10 x 10 km). In this modelling, we made the assumption that there is no direct sedimentary input by deep water channels coming from the Amazon deep turbidite system toward the distal channel system of the Orinoco. This assumption was done because, we do not have any direct available data which give evidence for the transport of siliciclastic sediments issued from the deep cone of the Amazon (Damuth et al., 1995; Flood et al., 1997; Normak et al., 1998; Pirmez and Imran, 2003; Jegou et al., 2008) connected with the deep water turbidite systems of the Orinoco. The potential connection between the Orinoco turbidite channels and the distal turbidite system of the Amazon would eventually corresponds to the depression of the Vema fracture zone (Baraza et al., 2000) but the bathymetric characteristics of the trough of the Vema fracture is not compatible with a simple gravity flow coming from the Amazon toward the Orinoco system and the channels present in the Vema fracture zone are clearly flowing toward the east (see accompanying digital figure 2). This is perfectly consistent with the measured bottom current of 1.1 Sv (1.1 10^6 m^3/s) toward the east in the Vema fracture zone which corresponds to the main flow of the Antarctic Bottom Water (AABW) entering the Demerara abyssal basin and flowing toward the east in the eastern Atlantic (McCoy, 1969; Molinari et al., 1992; Rhein et al., 1998; Demidov et al.2007; Morozov et al., 2008). Although a siliciclastic input from the deep water Amazon cone toward the Orinoco turbidite system is possible, for the best of our knowledge, there is no direct evidence for this. In this modelling, also because of the lack of concrete and precise data, we also did not take into account the possible contribution of an eventual branch of the deep Antartic Bottom Current in the hydraulic dynamics of the distal turbidite system of the Orinoco (see discussion above). Because of the reasons mentioned above, finally, we just tested in the modelling the simple hypothesis of a purely gravitational process for the deep Orinoco turbidite system development.

Taking into account the available data about water flow and sedimentary supply (see above), the mean upstream water fluxes issued from the Orinoco draining area chosen for the modelling was 35000 m^3/s, *i.e.* 1.1×10^{12} m^3/a (Warne et al., 2002) and it was kept constant during the whole modelling period. The solid sedimentary flux issued from the Orinoco platform (including both the Orinoco and the Guyana Coastal Current) toward the turbiditic system was estimated to be around to 210 x 10^6 metric ton/a (Van Andel, 1967; Milliman *et al.*, 1982; Rodriguez and Meade, 1983; Meade, 1990; Warne et al., 2002). This sedimentary flux was also kept constant during the whole modelling period

The time period considered for the stratigraphic modelling (50 ka to present) corresponds to the period of eustatic lowstand from 50 to 10 ka, and to a period of sea level rise between 10 ka and present time. The global eustatic variations modelled in this study were taken from Shen et al. (1995).

Results

The results of this numerical modelling show that the spatial distribution of the turbidite channel pattern is mostly controlled by the morphology of the seafloor and indeed can easily be compared with the real channel pattern described above and which actually follows the general natural line of greatest slope (Figs. 21, 22).

The modelling shows that during the period of low sea level (last glacial event between 50 and 10 ka) a complex multiple-channel turbidite system developed and the turbidite system propagated above the prism and in the abyssal plain generating a lowstand prograding complex. The model shows that the main sandy depocentres are located at the base of the upper continental slope above the tectonic prism and in the abyssal plain, at the front of the prism (Fig. 23) which is in perfect agreement with the available data. During this lowstand period, on the simulated Orinoco platform area, we note a high dispersion of the turbiditic flows. This induces relatively homogeneous concentration and velocity of the water fluxes on the platform area. This induces, on the shelf break, the development of several sub-parallel channels generating a multiple-source channel network. Above the prism, the global distribution of the channel pattern is very similar to the pattern observed on the acquired marine geophysical data with the focusing of the channels toward the front of the accretionary prism (Fig. 23). Moreover, at a very general scale, using the simple boundary conditions described above, the model is able to respect very faithfully the overall organization of the channel system, even in its distal parts. Notably, it shows that the distal system is getting around the Tiburon and Barracuda ridges in the Abyssal plain far away eastward of the front of the accretionary prism and connects with the Barracuda trough and the Puerto Rico trench (Fig. 22).

During the period from 10 ka to present which corresponds to the Holocene eustatic rise, the modelling shows that a drastic decrease of fluvial input to deepwater occurred. As a consequence of the sea level rise, a large accommodation space formed on the shelf confining sedimentation mostly on the Orinoco deltaic platform and producing a starvation downstream in areas of former turbidite sedimentation. This is also in very good agreement with the piston coring results which show superficial hemipelagic sedimentation in the deep water zones and an inactive phase of the deep turbidite system during recent times. The remaining water flow toward deep water is then partly deported toward the north-east of the platform, notably in a channel trending toward the north, sourcing the Barbados Basin, which is an isolated closed basin located above the Barbados accretionary prism (Fig. 24, 25).

DISCUSSION AND CONCLUSION

The data and the modelling presented here are both consistent to interpret the modern turbidite system as a gravity system mainly triggered by the natural slope. Also, this study, among others all around the world, outlines that sand-rich deposits are found very far away from their continental sources (see Cater, 1988; Saller et al., 2003; Flood and Damuth, 1987; Piper and Normak, 2001; Deptuck et al., 2007; Wynn et al., 2007; Shanmugam, 2012, and many others). In the case of the Orinoco turbidite system, we have shown that sand has transited along the channel system for more than 3000 km away from the shore of the Orinoco delta.

Also, whereas in most of the passive margins, turbidite systems are classically organized, upstream to downstream, as localized sources on the platform generating canyons at the shelf-edge and/or in the upper slope, then channel-levees, then lobes (like the neighbouring Amazon system for instance). Here, due to the control by active tectonics, the Orinoco turbidite system is organized upslope, as a multiple-source sand-rich system, then downslope as channel-levees and canyons bathymetrically confined in the deformation belt of the active margin, then as a very long-distance sand-rich channel system in the abyssal plain and in the subduction trench.

From a dynamic point of view, the data and the modelling suggest both that the main deposition processes in this system swing from distal long-distance deep sand transit and deposition during lowstands to proximal sand bars deposition mostly confined on the shelf during highstands. Indeed, from the available data, it seems that the deep turbidite system was most active during the last glacial event and it is currently in a low phase of activity since the recent Holocene rise of sea level. Nowadays, the sedimentation is largely located on the Orinoco delta platform and on the upper slope.

The interactions between tectonics and sedimentation in the east Caribbean active margin give a reference example to help to interpret modern systems in similar tectonic context but also older systems incorporated inside accretionary prisms. The modern Orinoco turbidite system is indeed very similar to ancient turbidite material, notably of Eocene age, incorporated within the accretionary prism as it has been shown from the outcrops of Chalky Mount onshore Barbados Island. Indeed, the study of the frontal accretionary processes at the modern front of the accretionary prism shows that the inner fan, the mid-fan and the outer-fan are all progressively incorporated within the tectonic wedge (Fig. 25). During the progressive migration of the deformation front, these elements containing excellent sandy layers were incorporated deeper and deeper into the accretionary wedge, the older and older they are (Fig. 18). The ancient turbidite system that can be observed onshore Barbados Island corresponds very probably to a mid-fan system deposited at the front of the early accretionary prism during Eocene times. Of course, what can be seen in the Barbados island is much more localized than what can be seen in the modern system but it shows characteristics totally similar to the mid fan of the present-day system and as such we can consider that both systems (ancient and recent) are very similar. Very probably, sand-rich deposits similar to the modern system can be found accreted at depth all over the Barbados prism.

Acknowledgements.

Special thanks are due to Philippe Joseph who contributed to the improvement of the initial manuscript and to the two reviewers who made very constructive comments to improve the manuscript.

REFERENCES CITED

Alfonso, J.A., Martinez M., Flores S., Benzo Z., 2006. Distribution of trace elements in offshore sediments of the Orinoco Delta. Journal of Coastal Research 22, 3, 502-510.

Anthony, E.J., Gardel, A., Gratiot, N., Proisy, C., Allison, M.A., Dolique, F., Fromard, F., 2010. The Amazon-influenced muddy coast of South America: A review of mud-bank–shoreline interactions Earth-Science Reviews 103, 99–121.

Aslan, A., White W., Warne A., Guevara E.H., 2003. Holocene evolution of the Western Orinoco delta, Venezuela. Geological Society of America Bulletin 115, 479-498.

Bader, R.G., Gerard, R.D., Benson, W.E., Bolli, H.M., Hay, W.W., Thomas Rothwell, W. Jr., Ruef, M.H., Riedel, W.R., and Sayles, F.L., 1970. Site 27, in Initial reports of the Deep Sea Drilling Project, Volume 4: Washington, D.C., U.S. Government Printing Office, 93–123.

Baraza, J., Ercilla, G. and the CAMEL shipboard party, 1997. The Equatorial Atlantic Mid-Ocean Channel: an ultra high-resolution image of its burial history based on TOPAS profiles. Marine Geophysical Researches 19, 2, 115-135.

Baraza, J., Ercilla, G., Chiocci, F.L., Casas, D., Estrada, F., Pérez-Belzuz M.F., Pérez-Belzuz, F.. 2000. El Canal Medio-Oceánico de Vidal (Atlántico Occidental- Ecuatorial): Características morfológicas y sísmicas. En Valles submarinos y sistemas turbidíticos modernos (Belén Alonso y Gemma Ercilla, eds.), CSIC, Barcelona 2000. 251-270.

Baumgartner, P.O., Flores, K., Bandini, A.N., Girault, F., Cruz, D., 2008. Upper Triassic to Cretaceous radiolaria from Nicaragua and Northern Costa Rica - The Mesquito Composite Oceanic Terrane. Ofioliti 33, 1-19.

Beck, C., Ogawa, Y., Dolan, J. 1990. Eocene paleogeography of the southeastern Caribbean: relations between sedimentation on the Atlantic abyssal plain at site 672 and evolution of the South America margin, in: Proc. ODP, Sci. Results ,Mascle, A., Moore, J.C., eds, 1990, College Station, TX, (Ocean Drilling Project), 110, 7-15.

Belderson, R.H., Kenyon N.H., Stride A.H., Pelton C.D., 1984. A "braided" distributary system on the Orinoco deep-sea fan. Marine Geology 56, 1-4, 195-206.

Brink, U.T., Danforth, W., Polloni, C., Andrews, B., Llanes, P., Smith, S., Parker, E., Uozumi, T. 2004. New seafloor map of the Puerto Rico trench helps assess earthquake and tsunami hazards. Eos 85, 37, 349-351.

Biju-Duval, B., P. Le Quellec, A. Mascle, V. Renard, P. Valery, 1982. Multi-beam bathymetric survey and high resolution seismic investigations on the Barbados ridge complex eastern Caribbean: a key to the knowledge and interpretation of an acrretionary wedge. Tectonophysics 80, 275-304.

Biju Duval, B., Moore, J.C., and Shipboard Scientific Party, 1984, Site 543: Oceanic reference site east of the Barbados ridge complex, in Initial reports of the Deep Sea Drilling Project, Volume 78A: Washington, D.C., U.S. Government Printing Office, 227–293, doi:10.2973/dsdp.proc.78a.

Biju-Duval B., Caulet J.P., Dufaure Ph., Mascle A., Muller C., Richert J.P., Valery P. 1985. The terrigenous and pelagic series of Barbados island: Paleocene to Middle Miocene slope deposits accreted to the lesser Antilles margin. Géodynamique des Caraïbes, Symposium, ed. Technip, 187-197.

Birch, F., 1970, The Barracuda fault zone in the western North Atlantic: Geological and geophysical studies: Deep-Sea Research, 17, 847–859.

Bouma, A .H. 1962. Sedimentology of some flysch deposits. Elsevier, Amsterdam, 168 pages.

Bouysse, P., Westercamp, D., Andreieff, P., 1990. The Lesser Antilles island arc. Proceedings of the Ocean Drilling Program, Scientific Results. 110, 29-44.

Brami, T. R., Pirmez C., Archie C., Heeralal S., Holman K.L., 2000. Late Pleistocene deep-water stratigraphy and depositional processes. Memoir of the GCSSEPM 20, 104-115.

Brown, K.M., Westbrook, G.K., 1987. The tectonic fabric of the Barbados ridge accretionary complex. Marine and Petroleum Geology 4, 71-81.

Brown, K.M., Mascle, A., Behrmann, J. 1990. Mechanisms of accretion and subsequent thickening in the Barbados ridge accretionary complex: balanced cross sections across the wedge toe. in: Proc. of the ODP, Sci. results., ed Moore, J.C., Mascle, A., et al., 1990, College Station, TX (Ocean J)rilling Program), 110, 209-227.

Calais, E., Y. Mazabraund, B. Mercier de Lepinay, P. Mann, G. Mattioli,, and, P. Jansma, 2002. Strain partitioning and fault slip rates in the northeastern Caribbean from GPS measurements. Geophysicsal Research Letters, 29, no. 18, 1856, doi:10:1029/2002GL015397.

Callec, Y., Deville, E., Desaubliaux, G., Griboulard, R., Huyghe, P., Mascle, A., Mascle, G., Noble, M., Padron De Carillo, C., Schmitz, J., 2010. The Orinoco turbidite system: Tectonic controls on Seafloor Morphology and Sedimentation. AAPG Bulletin 94, 6, 869-887.

Campan, A., 1995. Analyse cinématique de l'Atlantique équatorial: implications sur l'évolution de l'Atlantique sud et sur la frontière Amérique du Nord/Amérique du Sud. Thèse de doctorat de l'université Pierre et Marie Curie.

Cater, R.M., 1988. The nature and evolution of deep-sea channel systems. Basin Research, 1, 41-54.

Chennouf, T. 1987. La terminaison sud de la ride de la Barbade (Marge active des Petites Antilles). Étude des relations tectonique sédimentation par application de la stratigraphie sismique. Thèse de l'Univ. P. et M. CURIE, Sciences de la Terre, Option: Géophysique appliquée, 198 pages.

Covault, Jacob A., and Stephan A. Graham. "Submarine fans at all sea-level stands: Tectono-morphologic and climatic controls on terrigenous sediment delivery to the deep sea." Geology 38.10 (2010): 939-942.

Curtin, T.B., 1986. Physical observation in the plume region of the Amazon river during peak discharge—II. Water masses. Continental Shelf Research 6, 53–71.

Damuth, J.E. 1975. Echo-character of the western equatorial Atlantic floor and its relationship to the dispersal and distribution of terrigenous sediments. Marine Geology 18, 17-45.

Damuth, J.E., Flood, R.D., Pirmez, C., Manley, P.L., 1995. Architectural elements and depositional processes of Amazon Deep-sea Fan: imaging by long-range sidescan sonar (GLORIA), bathymetric swath-mapping (Sea Beam), high-resolution seismic and piston-core data. In: Pickering, K.T., Hiscott, R.N., Kenyon, N.H., Lucchi, F.R., Smith, R.D.A. (Eds.), Atlas of Deep-water Environments: Architectural Styles in Turbidite Systems. Chapman and Hall, London, 105–121.

DeMets, C., Gordon, R.G., Argus, D.F., and Stein S., 1990, Current plate motions: Geophysical Journal International, 101, 425–478, doi:10.1111/ j.1365-246X.1990.tb06579.x.

DeMets, C., Jansuma, P.E., Mattioli, G.S., Dixon, T.H., Farina-Fred, Bilham, R., Calais, E., Mann, P. 2000. "GPS geodetic constraints on Caribbean-North America Plate motion". Geophysical Research Letters 27, 3, 437-440.

Demidov, A.N., Dobrolyubov, S.A., Morozov, E.G., Tarakanov, R.Y., 2007. Transport of bottom waters through the Vema fracture zone in the Mid-Atlantic Ridge. Doklady Earth Sciences 416, 7, 1120-1124.

Deptuck, M.E., Z. Sylvester, C. Pirmez, and C. O'byrne, 2007, Migration-aggradation history and 3-D seismic geomorphology of submarine channels in the Pleistocene Benin-major Canyon, western Niger Delta slope. Marine and Petroleum Geology, 24, 406-433.

Deville, E., Mascle, A., Guerlais, S.-H., Decalf, C., Colletta B. 2003. Lateral changes of frontal accretion and mud volcanism processes in the Barbados accretionary prism and some implications. In : C. Bartonini, R.T. Buffler and J. Blickwede, Eds. The circum-Gulf of Mexico and the Caribbean. Hydrocarbon habitats, basin formation, and plate tectonics. AAPG memoir 79, The Circum-Gulf of Mexico and the Caribbean:Mexico and the Caribbean Region Hydrocarbon Habitats, Basin Formation, Plate Tectonics. Cl. Bartolini, T. Buffler, J.F. Blickwede, eds., Chapter 30, 1-19.

Deville, E., Callec, Y., Desaubliaux, G., Mascle, A., Huyghe, P., Griboulard, R., Noble, M., 2003. Deep-water erosion processes in the Orinoco turbidite system: Offshore October 2003, Offshore-Conroe-Tex., 63, 10, 92-96.

Deville, E., Battani, A., Griboulard R., Guerlais S.H., Lallemant S., Mascle A., Prinzhofer A., Schmitz J., 2004. Processes of Shale Diapirism and Mud Volcanism in the Barbados-Trinidad Compressional System: Integrated Structural, Thermal and Geochemical Approach. Memoir of the GCCSEPM 24, 514-527.

Deville, E., Guerlais, S.-H., Callec, Y., Griboulard, R., Huyghe, P., Lallemant, S., Mascle, A., Noble, M., Schmitz, J. and the Caramba working group, 2006. Liquefied vs Stratified Sediment

Mobilization Processes: Insight from the South of the Barbados Accretionary Prism. Tectonophysics 428, 33-47.

Deville É., Mascle A., 2012. The Barbados Ridge: A mature Accretionary Wedge in Front of the Lesser Antilles Active Margin. Special Volume: Principles of Geologic Analysis DOI: 10.1016/B978-0-444-53042-4.00021-2, Elsevier, A.W. Bally and D.G. Roberts eds., Chapter 21, 581-607.

Di Crocce, J,, Bally, A.W., Vail, P., 1999. Sequence stratigraphy of the eastern Venezuelan Basin, Caribbean Basins. in Sedimentary Basins of the World, 4 edited by P. Mann (Series Editor: K.J. Hsû), 419-476.

Diaz de Gamero, M. L., 1996. The changing course of the Orinoco River during the Neogene: A review. Palaeogeography, Palaeoclimatology, Palaeoecology, 123, 385–402.

Dixon, T.H., Mao, A.L., 1997. A GPS estimate of relative motion between North and South America. Geophysical Research Letters 24, 535–538, doi:10.1029/97GL00284.

Dupuis, V., 1999: Origine et mise en place de témoins accrétés du plateau océanique caraïbe crétacé en République Dominicaine (Grandes Antilles). Unpublished PhD thesis, University of Lausanne, p. 239.

Embley R. W., Langseth, M., 1977. Sedimentation processes on the continental rise of northeastern South America. Marine Geology 25, 279-297.

Embley, R.W., Ewing, J.I., Ewing, M., 1970. The Vidal deep-sea channel and its relationship to the Demerara and Barracuda abyssal plains: Deep Sea Research and Oceanographic Abstracts, 17, 539–552, doi:10.1016/0011-7471(70)90066-5.

Ercilla, G., Alonso B., Baraza J., Casas D., Chiocci F L., Estrada F., Farran M., Gonthier E., Perez-Belzuz F., Pirmez C., Reeder M., Torres J., Urgeles R., 1998. New high-resolution acoustic data from the "braided system" of the Orinoco deep-sea fan. Marine Geology 146, 1-4, 243-250.

Ercilla, G., Alonso, B., Baraza, J., 2000. High resolution morpho-sedimentary characteristics of the distal Orinoco turbidite system. GCSSEPM Foundation 20th Annual Research Conference, Deep-Water Reservoirs of the world, 374-388.

Ercilla, G., Alonso B., Estrada F., Chiocci F L., Baraza J., Farran M., 2002. The Magdalena turbidite system (Carribean Sea): Present-day morphology and architecture model. Marine Geology 185, 303-318.

Erlich, B., 1992. Petroleum geology of the Eastern Venezuela Foreland basins. in McQueen, Leckie ed. Foreland basins and Fold belts, AAPG Mem. 55, 341-362.

Faugeres, J. C., Gonthier, E., Masse, L., Parra M., Pons, J. C., Pujol, C., 1991. Quaternary deposits and canyons on the South Barbados accretionary prism. Marine Geology 96, 247-267.

Faugeres, J. C., Gonthier, E., Griboulard, R., Masse L., 1993. Quaternary sandy deposits and canyons on the Venezuelan margin and South Barbados accretionary prism. Marine Geology 110, 1-2, 115-142.

Ferguson, I.J., Westbrook, G.K., Lanseth, M.G., Thomas, G.P.,1993. Heat flow and thermal models of the Barbados Ridge accretionary complex. Journal of Geophysical Research 98, 4121-4142.

Flood, R.D., Damuth, J.E., 1987. Quantitative characteristics of sinuous distributary channels on the Amazon deep-sea fan. Geological Society of America Bulletin 98, 728–738.

Franzinelli, E., Potter, P.E., 1983. Petrology, chemistry, and texture of modern river sands, Amazon River system. Journal of Geology 91, 23–39.

Galbraith, R.M., Brown, A.R., 1999. Field appraisal with three-dimensional seismic surveys offshore Trinidad. in: Interpretation of three-dimensional seismic data. AAPG Memoir 42, 318-323.

Garcia, D., Joseph, P., Marechal, B., Moutte, J., 2004. Patterns of geochemical variability in relation to turbidite facies in the Grès d'Annot Formation. In : Joseph P. and Lomas S.A.(eds). " Deep-Water Sedimentation in the Alpine Basin of SE France: New perspectives on the Grès d'Annot and related systems ", Geological Society, London, Special Publications, 221, p. 349-365.

Gersztenkorn, A., Sharp, J., Marfurt, K., 1999. Delineation of tectonic features offshore Trinidad using 3-D seismic coherence. Society of Exploration Geophysicists. The Leading Edge, 18; 9, 1004-1008.

Gibson, R.G., Bentham, P.A., 2003. Use of fault-seal analysis in understanding petroleum migration in a complexly faulted anticlinal trap, Columbus Basin, offshore Trinidad: in: Fault seals. Davies-Russell-K (editor); Handschy-James-W (editor), AAPG Bulletin, 87, 3, 465-4783.

Gonthier, E., Faugères, J. C., Bobier, C., Griboulard, R., Huyghe, P., Massé, L., Pujol C., 1994. Le prisme d'accrétion tectonique Sud-Barbade. Revue Aquitaine Océan, 1, 105 pages.

Gordon, R.G., 1998. The plate tectonic approximation: Plate non rigidity, diffuse plate boundaries, and global plate reconstructions. Annual Review of Earth and Planetary Sciences, 26, 615–642, doi:10.1146/annurev.earth.26.1.615.

Granjeon, D., Joseph, P., 1999. Concepts and applications of a 3D multiple lithology, diffusive model in stratigraphic modelling. In : Harbaugh J.W. & al. (eds) Numerical experiments in stratigraphy, SEPM Sp. Pub. 62.

Harris, P.T. , Whiteway, T., 2011. Global distribution of large submarine canyons. Marine Geology 285, 69–86.

Henry, P., Le Pichon, X., Lallemant, S., Foucher, J.P., Westbrook, G.K., Hobart, M.A. 1990. Mud volcano field seaward of the Barbados accretionary complex: a deep towed side scan sonar survey. Journal of Geophysical Research, 95, B6, 8917-8929.

Heppard, P.D., Cander, H.S., Eggertson, E.B., 1998. Abnormal pressure and the occurrence of hydrocarbons in offshore eastern Trinidad, West Indies. AAPG Memoir 70, 215-246.

Herrera, L., Febres, G., Avila, R., 1981. Las mareas en aguas Venezolanas y su amplificacion en la region del delta del Orinoco. Acta Cientifica Venezolana, 32, 299–306.

Hill, R.J., Schenk, C.J., 2005. Petroleum geochemistry of oil and gas from Barbados: Implications for distribution of Cretaceous source rocks and regional petroleum prospectivity. Marine and Petroleum Geology 22, 917–943.

Huyghe, P., Griboulard, R., Faugeres, J.C., Gonthier, E., Bobier, C., 1996. Géométrie des bassins transportés à l'aplomb de la terminaison méridionale du prisme de la Barbade. Bull. Soc. Géol.. Fr. 167, 3, 348-359.

Huyghe, P., J.L. Mugnier, R. Griboulard, Y. Deniaud, E. Gonthier, and J.C. Faugères, 1999, Review of the tectonic control and sedimentary patterns in Late Neogene piggyback basins on the Barbados ridge complex, Caribbean Basins: Sedimentary Basins of the World, 4 edited by P. Mann (Series Editor: K.J. Hsü), 369-388.

Huyghe, P., Foata M., Deville E., Mascle G. and the Caramba Working Group, 2004. Channel profiles through the active thrust front of the southern Barbados prism. Geology 32, 5, 429-432.

Jansma, P., Lopez A., Mattioli G., DeMets C., Dixon T.,Mann P., Calais, E., 2000. Microplate tectonics in the northeastern Caribbean as constrained by Global Positioning (GPS) geodesy. Tectonics 19, 1021-1037.

José Méndez, B., 2000. Delta de Orinoco (Geologia). Instituto Nacional de Geologia y mineria ingeomin. Boletin de geologia. Publicacion especial, n°13, 127 pages.

Joseph, P., Callec, Y., Ford M., 2012. Dynamic Controls on Sedimentology and Reservoir Architecture in the Alpine Foreland Basin. A Field Guide to the Eocene-Oligocene Grès d'Annot Turbidite System of SE France. IFP Energies nouvelles e-books. DOI:10.2516/ifpen/2012001 http://books.ifpenergiesnouvelles.fr.

Kasper D.C., Larue D.K. 1986. Paleogeographic and tectonic implications of quartzose sandstones of Barbados, Tectonics 5, 837-854.

Klitgord, K.D., Schouten, H., 1986, Plate kinematics of the central North Atlantic, in Vogt, R., and Tucholke, B.E., eds., The western North Atlantic region: Boulder, Colorado, Geological Society of America, Geology of North America, M, 351–404.

Larue D.K., Provine K.G. 1988. Vacillatory turbidites, Barbados. Sedimentary Geology 57, 211-219.

Larue D.K., Speed R.C. 1983. Quartzose turbidites of the accretionary complex of Barbados, I: Chalky Mount succession. Journal of sedimentary Petrology 53, 4, 1337-1352.

Loncke, L., Droz, L., Gaullier, V, Basile, C., Patriat, M., Roest W., 2009. Slope instabilities from echo-character mapping along the French Guiana transform margin and Demerara abyssal plain. Marine and Petroleum Geology 26 , 5 , 711-723.

López, A. Stein, S., Dixon, T., Sella, G., Calais, E., Jansma, P., Weber, J., LaFemina, P. 2006. Is there a northern Lesser Antilles forearc block? Geophysical Research Letters. 33, 7.

Mac Coy, F.W., 1969. Bottom currents in the western Atlantic ocean between the Lesser Antilles and the Mid-Atlantic ridge. Deep-Sea Research, 16, 179-184.

Mann, P., 1999. Caribbean sedimentary basins: Classification and tectonic setting from Jurassic to Present, Chapter 1 in Caribbean Basins, 4: Sedimentary Basins of the World, edited by P. Mann, Elsevier, Amsterdam, 3-31.

Mann, P., E. Calais, J-C. Ruegg, C. DeMets, P. Jansma, G. Mattioli, 2002. Oblique collision in the northeastern Caribbean from GPS measurements and geological observations. Tectonics 21, 6, 1057, doi:10.1029.2001TC001304.

Mascle, A., Moore, J.C. 1990. ODP Leg 110: Tectonic and hydrologic synthesis. Proceedings of the Ocean Drilling Program, Scientific Results 110, 409-422.

Mascle, A., Endignoux, L., Chennouf, T. 1990. Frontal accretion and piggyback basin development at the southern edge of the Barbados ridge accretionary complex, in: Proc. of the ODP, Sci. results, eds MOORE, J.C., MASCLE, A., et al., 1990, College Station, TS (Ocean Drilling Program), Ocean Drilling Project, 110, pp 17-28.

Mascle, A., Moore, J.C., and Shipboard Scientifi c Party, 1988, Site 672, in Proceedings of the Ocean Drilling Program, Part A, Initial report, Volume 110: College Station, Texas, Ocean Drilling Program, 205–310.

Mattson, P. H., Pessagno, E.A. Jr. 1979. Jurassic and Early Cretaceous radiolarians in Puerto Rican ophiolite – Tectonic implications. Geology 7, 440-444.

Meade, R.H., 1990. Suspended sediments of the modern Amazon and Orinoco rivers: In: Quaternary of South America. Iriondo-Martin editor: Quaternary International, 21., 29-39.

Metcali, W.G., 1968. Shallow currents along the northeastern coast of South America. Journal Marine Research, 26, 232-243.

Milliman, J.D., Butenko, J., Barbot, J.P., Hedberg, I., 1982. Depositional patterns of modern Orinoco/ Amazon muds on the northern Venezuelan shelf. Journal of Marine Research 40, 3, 643-657.

Minster, J.B., Jordan, T.H., 1978. Present-day plate motions: Journal of Geophysical Research, 83, 5331–5354, doi:10.1029/JB083iB11p05331.

Molinari, R.L., Fine, R.A., Johns, E. 1992. The deep western boundary current in the tropical North Atlantic ocean. Deep-Sea Research 39, 11/12, 1967-1984.

Moore, J.C., Biju-Duval, B., 1982. Offscraping and underthrusting of sediment at the deformation front of the Barbados ridge: DSDP Leg 78 A. Geological Society of America Bulletin, 93, 1065-1077.

Moore, J.C., Bilju-Duval, B., 1984. Tectonic synthesis, DSDP leg 78 A: structural evolution of offscraped and underthrust sediment, northern Barbados ridgc complex, in: Initial Reports of the Deep Sea Drilling Project., ed B. Biju-Duval, Moore et al., U.S. Govt. Printing Office, Washington, 78 A, 601-621.

Moore J.C., Mascle A. and the scientific staff of ODP leg 110. 1988. Tectonics and hydrogeology of the northern Barbados Ridge: Results from Ocean drilling Program Leg 110. Geological Society of America bulletin, 100, 1578-1593.

Morozov E. G., A. N. Demidov, R. Yu. Tarakanov, 2008. Transport of Antarctic Waters in the Deep Channels of the Atlantic Ocean. Doklady Earth Sciences 423, 8, 1286–1289.

Moscardelli, L., L. Wood, P. Mann, 2006. Mass-transport complexes and associated processes in the offshore area of Trinidad and Venezuela. AAPG Bulletin 90, 7, 1059-1088.

Moscardelli, L, Wood L.J., Dunlap D.B., 2012. Shelf-edge deltas along structurally complex margins: A case study from eastern offshore Trinidad. AAPG Bulletin 96, 8, 1483–1522

Müller, R.D., Smith, W., 1993. Deformation of the oceanic crust between the North American and South American plates. Journal of Geophysical Research 98, 8275–8291, doi:10.1029/92JB02863.

Mutti, E., 1992, Turbidite sandstones. *in* E. Mutti, (ed.), AGIP Italy, 275 pages.

Padron de Carillo, C., 2008. Les interactions tectonique sédimentation entre le front du prisme de la Barbade et le delta de l'Orénoque, Géologie Alpine, Mémoire H.S. n°8 , 116 pages.

Padron de Carillo, C., E. Deville, P. Huyghe, S. Lallemant, J.F. Lebrun, A. Mascle, G. Mascle, M. Noble, and J. Schmitz (submitted). From Subduction to a Compressional transform system: Diffuse Deformation Processes at the Southeastern Boundary of the Caribbean Plate: Journal of Geophysical Research.

Paola, C., Heller, P.L., Angevine, C.L., 1992. The large scale dynamics of grain-size variation in alluvial basins, 1: theory. Basin Res., 4, 73–90.

Patriat, M., Pichot, T., Westbrook, G.K., Umber, M., Deville, E., Bénard, F., Roest, W., Loubrieu, B. and the ANTIPLAC cruise party 2011. Evidence for Quaternary convergence between the North American and South American plates, east of the Lesser Antilles. Geology 39, 979-982. doi: 10.1130/G32474.1.

Pichot, T., Patriat, M., Westbrook, G.K., Nalpas, T., Gutscher, M.A., Roest, W.R., Deville, É., Moulin, M., Aslanian, D., Rabineau, M., 2012. Tectono-sedimentary evolution of the Barracuda and Tiburon Ridges as recorded by Cenozoic stratigraphy, east of the Barbados accretionary wedge. Marine Geology 303-306, 154-171.

Pindell, J., Kennan, L., Stanek, K.P., Maresch, W.V., Draper G., 2006. Foundations of Gulf of Mexico and Carribean evolution : eight controversies resolved. Geologica Acta 4, 1-2, 303-341.

Piper, D.J.W., Normark, W.R., 2001. Sandy fans—from Amazon to Hueneme and beyond. Bulletin of the American Association of Petroleum Geologists 85, 1407–1438.

Pirmez, C., Flood, R.D., 1995. Morphology and structure of Amazon Channel. In: Flood, R.D., Piper, D.J.W., Klaus, A., et al. (Eds.), Proceedings of the Ocean Drilling Program, Initial Reports, 155,

Pirmez, C., Imran, J., 2003. Reconstruction of turbidity currents in Amazon Channel. Marine and Petroleum Geology 20, 823–849.

Postma, G., van Den Berg van Saparoea, A.-P., 2007. Flume modelling of river-delta systems at geological relevant time scales: templates for sea-level induced flux. In: Analogue and Numerical Forward Modelling of Sedimentary Systems; from Understanding to Prediction (Ed. by de Boer

P.L., Postma G., van der Zwan C.J., Burgess P.M. & Kukla P.) Int. Assoc. Sedim. Spec. Publ., 40, 191–206.

Postma, G., Kleinhans, M.G., Meijer, P.T., Eggenhuisen, J.T., 2008. Sediment transport in analogue flume models compared with real-world sedimentary systems: a new look at scaling evolution of sedimentary systems in a flume. Sedimentology, 55, 1541–1557.

Pudsey C.J., Reading H.C 1982. Sedimentology and structure of the Scotland Group, Barbados. In Trench and Forearc Geology (Ed. J.K. Leggett), Spec. Publ. Geol. Soc. London 10, 291-308.

Reading, H.G., Richards, M., 1994. Turbidite systems in deep water basin margins classified by grain size and feeder system. Bull. Am. Ass. Petrol. Geol. 78, 792-822.

Rhein, M., Stramma L., L., Krahmann, G., 1998. The spreading of Antarctic battom water in the tropical Atlantic. Deep-Sea Research, I, 45, 507-527.

Rodriguez, I.I., Meade, R.H., 1983. Hydrology of the Amazon and Orinoco rivers: Eos, Transactions, American Geophysical Union. 64, 45, 657.

Roest, W. R., Collette, B. J., 1986. The Fifteen-Twenty fracture zone and the North American-South American plate boundary. Journal of the Geological Society of London. 143, 5, 833-843, doi:10.1144/gsjgs.143.5.0833.

Roest, W.R., 1987, Seafloor spreading pattern of the North Atlantic between 10° and 40° N. Geologica Ultraiectina 48, 121 pages.

Ruiz M., Galve A., Monfret T., Sapin M., Charvis P., Laigle M., Evain M., Hirn A., Flueh E., Gallart J., Diaz J., Lebrun J.F. and The Lesser Antilles Thales scientific party, in press. Seismic activity offshore Martinique and Dominica islands (Central Lesser Antilles subduction zone) from temporary onshore and offshore seismic networks. Tectonophysics.

Rutledge, A.K., Leonard, D.S., 2001, Role of multibeam sonar in oil and gas exploration and development: Offshore Technology Conference 12956, 12 pages.

Saller, A.H., Noah, J.T., Ruzuar, A.P., and Schneider, R., 2004, Linked lowstand delta to basin-floor fan deposition, offshore Indonesia: an analog for deep-water reservoir systems: AAPG Bull., 88, 21–46.

Saunders, J.B., Bernoulli, D., Muller-Merz, E., Oberhaensli, H., Perch-Nielsen, K., Riedel, W.R., Sanfilippo, A., Torrini, R. 1984. Stratigraphy of late Middle Eocene to Early Oligocene in Bath cliff section, Barbados, West Indies. Micropaleontology, 30, 390-425.

Schmitz, M., Chalbaud D., Castillo J., Izarra C., 2002. The crustal structure of the Guayana Shield, Venezuela, from seismic refraction and gravity data Original Research Article Tectonophysics 345, 1–4, 103-118.

Senn, A., 1940. Paleogene of Barbados and its bearing on history and structure of Antillean-Caribbean region. Bulletin of the American Association of Petroleum Geologists 24, 9, 1548-1610.

Shanmugam, G., 2012. New Perspectives on Deep-water Sandstones. Origin, Recognition, Initiation, and Reservoir Quality. Elsevier, ISBN: 9780444563354, 544 pages.

Shen, J., Farrell, J.W., Murray, D.W., Warren, L.P., 1995. Timescale and Paleoceanographic implications of a 3.6 m.y. Oxygen record from the northeast Indian Ocean (Ocean Drilling Program Site 758). Paleoceanography, vol. 10, 1, p 21-47.

Speed, R.C., Barker L.H., Payne P.L.B., 1991. Geologic and hydrocarbon evolution of Barbados. Journal of petroleum Geology, 14 (3), 323-342.

Stephan, J.F., Mercier De Lepinay, B., Calais, E., Tardy, M., Beck, C., Carfantan, J.C., Olivet, J.L., Vila, J.M., Bouysse, P., Mauffret, A., Bourgeois, J., Thery, J.M., Tournon, J., Blanchet, R., Dercourt, J., 1990. Paleogeodynamic maps of the Carribean: 14 steps from Lias to Present. Bull. Soc. Géol. de France, VI, 6, 915-919.

Stride, A.H., Belderson, R.H., Kenyon, N.H., 1982. Structural grain, mud volcanoes and other features on the Barbados ridge complex revealed by Gloria long-range side-scan sonar. Marine Geology 49, 187- 196.

Sumner, R.H., Westbrook, G.K., 2001. Mud diapirism in front of the Barbados accretionary wedge: The infl uence of fracture zones and North America– South America plate motions: Marine and Petroleum Geology, 18, 591–613, doi:10.1016/S0264-8172(01)00010-1.

Tucholke, B.E. 2002. The Greater Antilles Outer Ridge: development of a distal sedimentary drift by deposition of fine-grained contourites. Geological Society, London, Memoir 22, 39-55, doi:10.1144/GSL.MEM.2002.022.01.04.

Van Andel, T.J., 1967. The Orinoco River. Journal of Sedimentary Petrology, 37 2, 297-310.

Veeken, P.C.H., 1983. Guyana basin, offshore Northeast South America, in: Seismic expression of structural styles, a picture and work atlas. AAPG, studies in Geology série 15, 2,

Warne, A.G., R.H. Meade, W.A. White, E.H. Guevara, J. Gibeaut, R.C. Smyth, A. Aslan, T. Tremblay, 2002. Regional controls on geomorphology, hydrology, and ecosystem integrity in the Orinoco delta, Venezuela. Geomorphology 44, 3-4, 273-307.

Weber J.C., T.H. Dixon, C. De Mets, W.B. Ambeth, P. Jansma, G. Mattioli, J. Saleh, G. Sella, R. Bilham, and O. Perez, 2000, GPS estimate of relative motion between the Caribbean and South American plates, and geologic implications for Trinidad and Venezuela. Geology 29, 1, 75-78.

Westbrook, G.K., 1975. The structure of the crust and upper mantle in the region of Barbados and the Lesser Antilles. Journal of Royal Astronomic Society, 43, pp.201-242.

Westbrook, G. K. 1982. The Barbados Ridge Complex, tectonics of a mature forearc system. Sedimentation and tectonics in ancient and modern active plate margins. ed Leggett, J.K.,Special Publication Geological Society of London 10, 275-290.

Westbrook, G.K., Smith, M.J., Peacock, J.H., Poulter, M.J. 1982. Extensive underthrusting of undeformed sediment beneath the accretionary complex of the Lesser Antilles subduction zone. Nature, 300, 625-628.

Westbrook, G.K., Smith, M.J. 1983. Long decollements and mud volcanoes: evidence from the Barbados ridge complex for the role of high pore fluid pressure in the developement of an accretionary complex. Geology, 11, 279-283.

Westbrook, G.K., 1984, Magnetic lineations and fracture zones, in Speed, R.C., et al., eds., Lesser Antilles Arc and adjacent terranes: Ocean Margin Drilling Program regional atlas series, Volume 10: Woods Hole, Massachusetts, Marine Science International, sheet 5.

Westbrook, G.K., Mascle, A., Biju-Duval, B. 1984. Geophysics and the structure of the Lesser Antilles Forearc, in: Initial Reports of the Deep Sea Drilling Project, ed B. Biju-Duval, Moore et al., U.S. Govt. Printing Office, Washington, 78 A, 23-38.

Westbrook, G.K., Ladd, J.W., Buhl, P., Bangs, N., Tiley, G.J. 1988. Cross-section of an accretionary wedge. Barbados Ridge complex. Geology, 16, 7, 631-635.

Wood, L.J., 2000. Chronostratigraphy and tectonostratigraphy of the Columbus Basin, eastern offshore Trinidad. AAPG Bulletin, 84, 12, 1905-1928.

Wright, A., 1984. Sediment distribution and depositional processes operating in the Lesser Antilles intraoceanic island arc, Eastern Caribbean. in: Biju-Duval, Moore et al., Init. Rep. Deep Sea Drill. Proj., U. S. govt. Printing Office, Washington, 78A, 23-38.

Wynn, R.B., Cronin, B.T., Peakall, J. 2007 Sinuous deep-water channels: Genesis, geometry and architecture. Marine and Petroleum Geology 24, 6-9, 341-387.

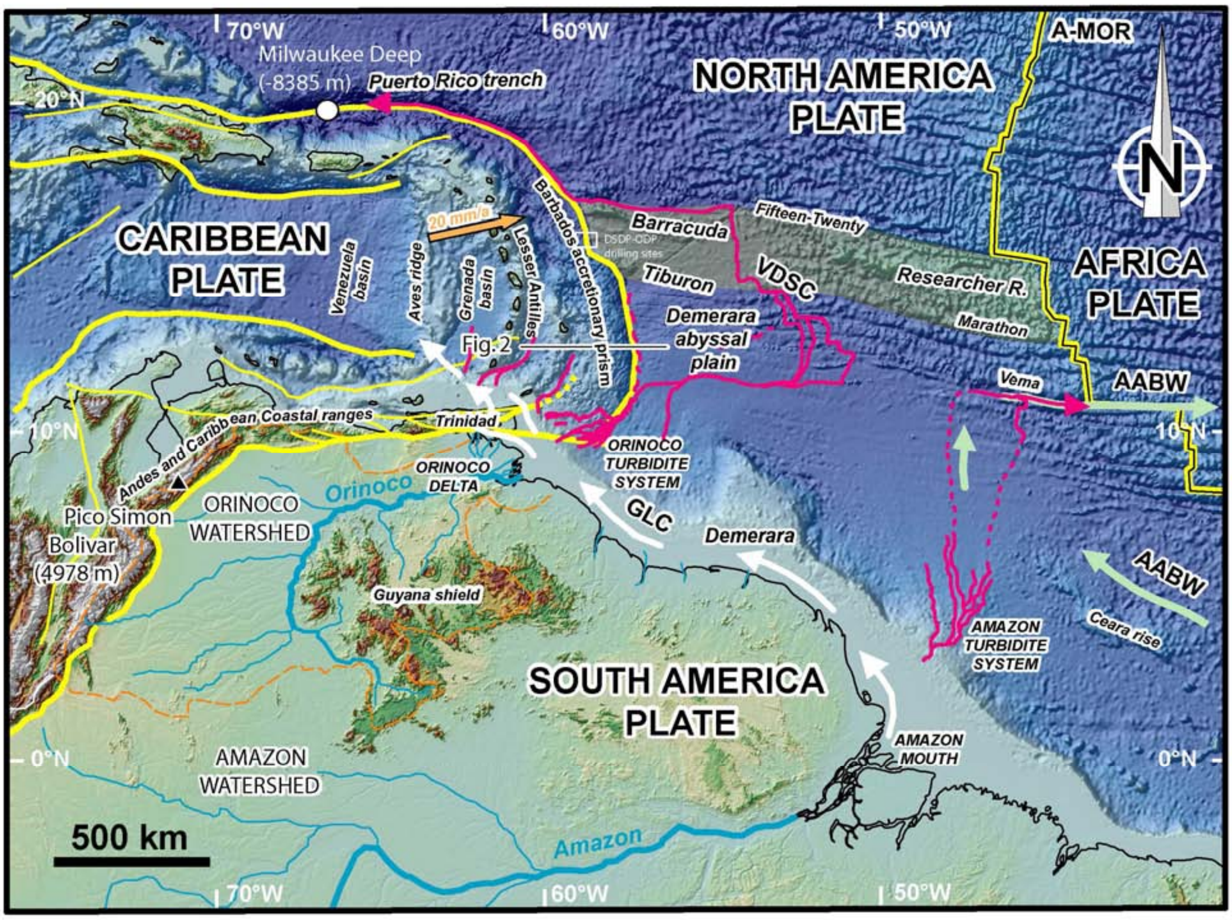

Figure 1 – General sketch-map of the Orinoco siliciclastic system showing its close interaction with the compressional front of the Caribbean plate. Orange arrow: vector displacement of the Caribbean Plate with respect to the North American Plate. Red lines and arrows: turbidite systems; AABW: Antarctic Bottom Water (Green arrows; location from Rhein et al., 1998); GLC: Guyana Littoral Current (white arrows); VDSC: Vidal Deep Sea Channel. A-MOR: Atlantic Mid-Oceanic Ridge.

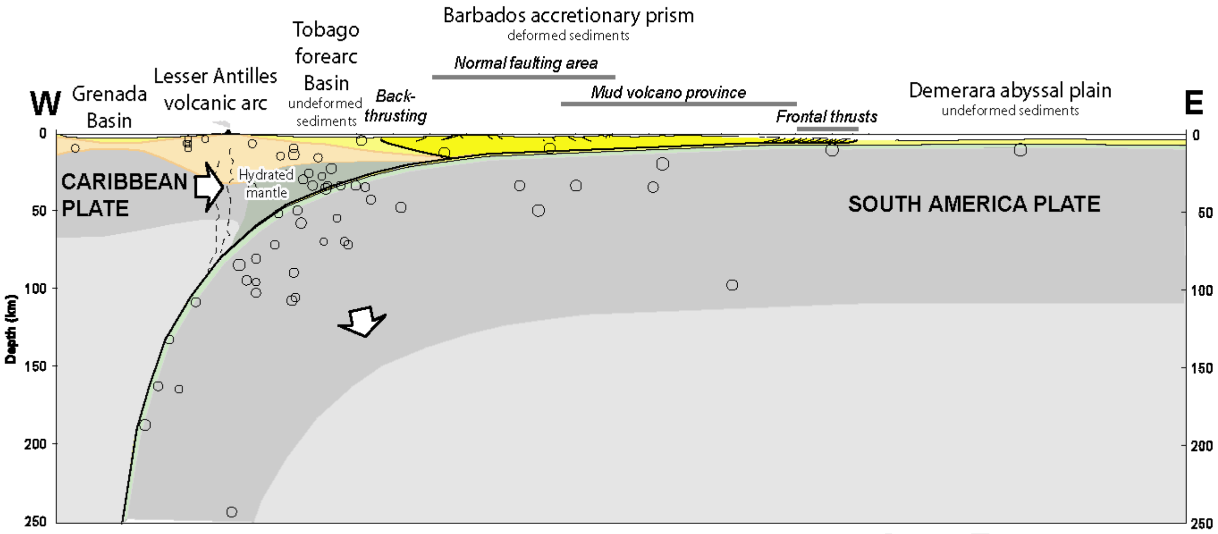

Figure 2 – E-W cross-section across the east Caribbean subduction zone (Location on figure 1).

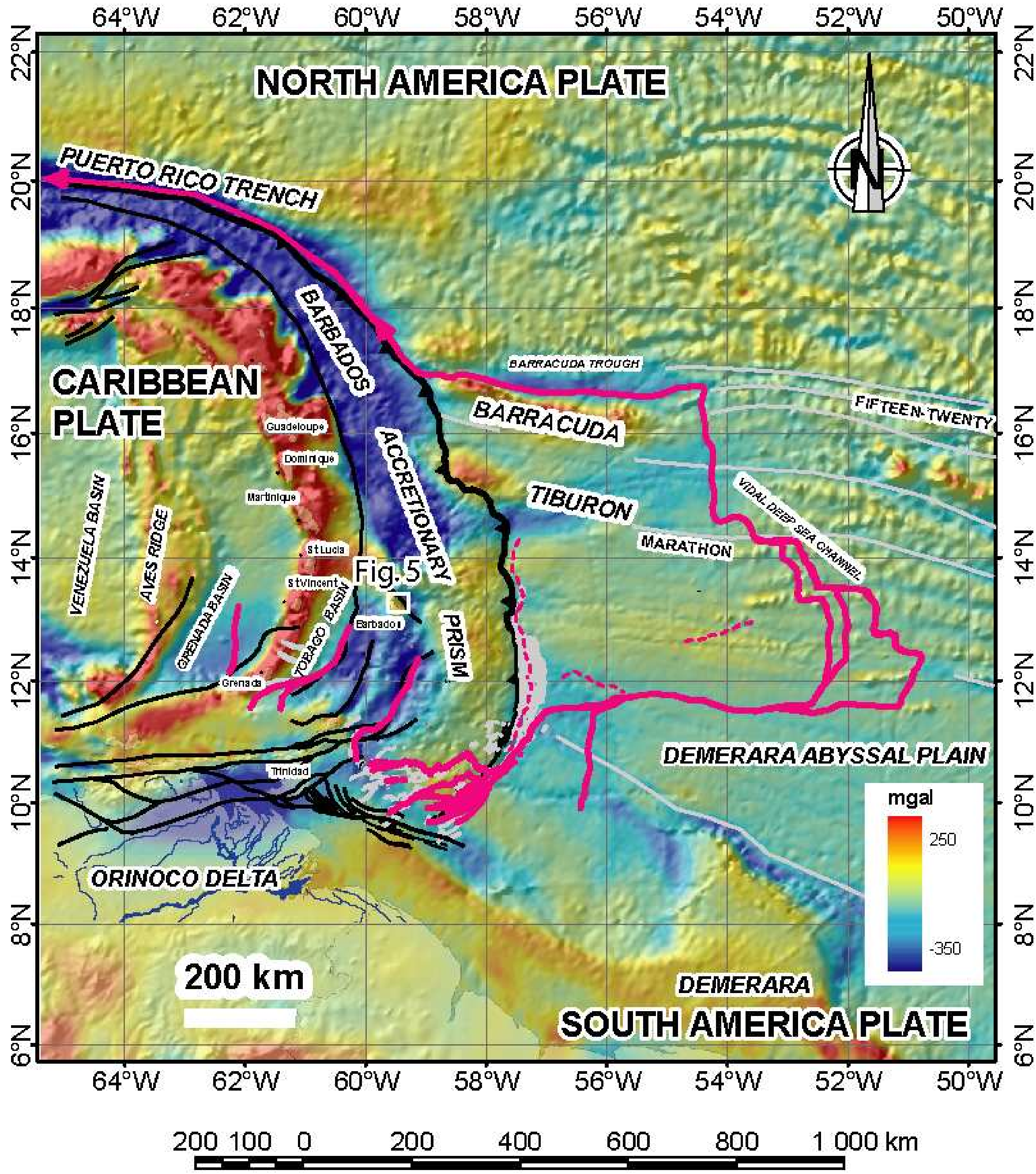

Figure 3 – Gravimetric map outlining the location of the main sedimentary accumulations. Note that the trough north of the Barracuda ridge is sourced from the east by the distal turbidite system of the Orinoco.

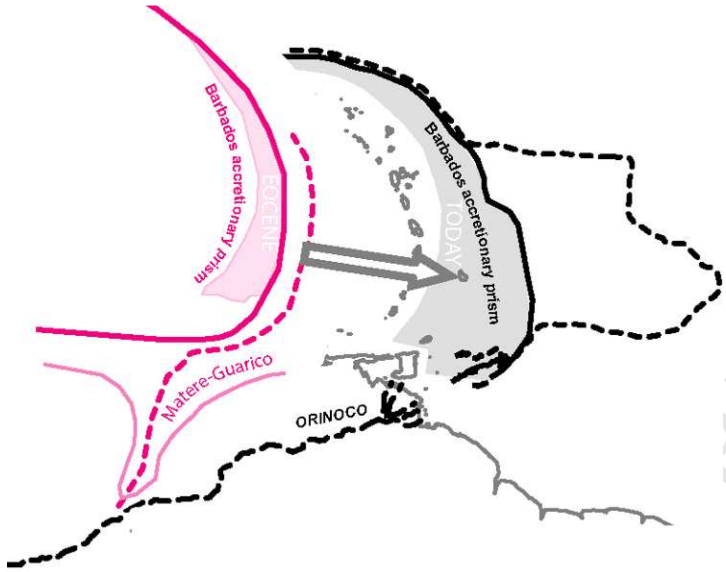

Figure 4 – Displacement of the Barbados accretionary prim and the Orinoco deposition system from Eocene times (pink) to present (black). Eocene restoration from Stephan et al. (1990).

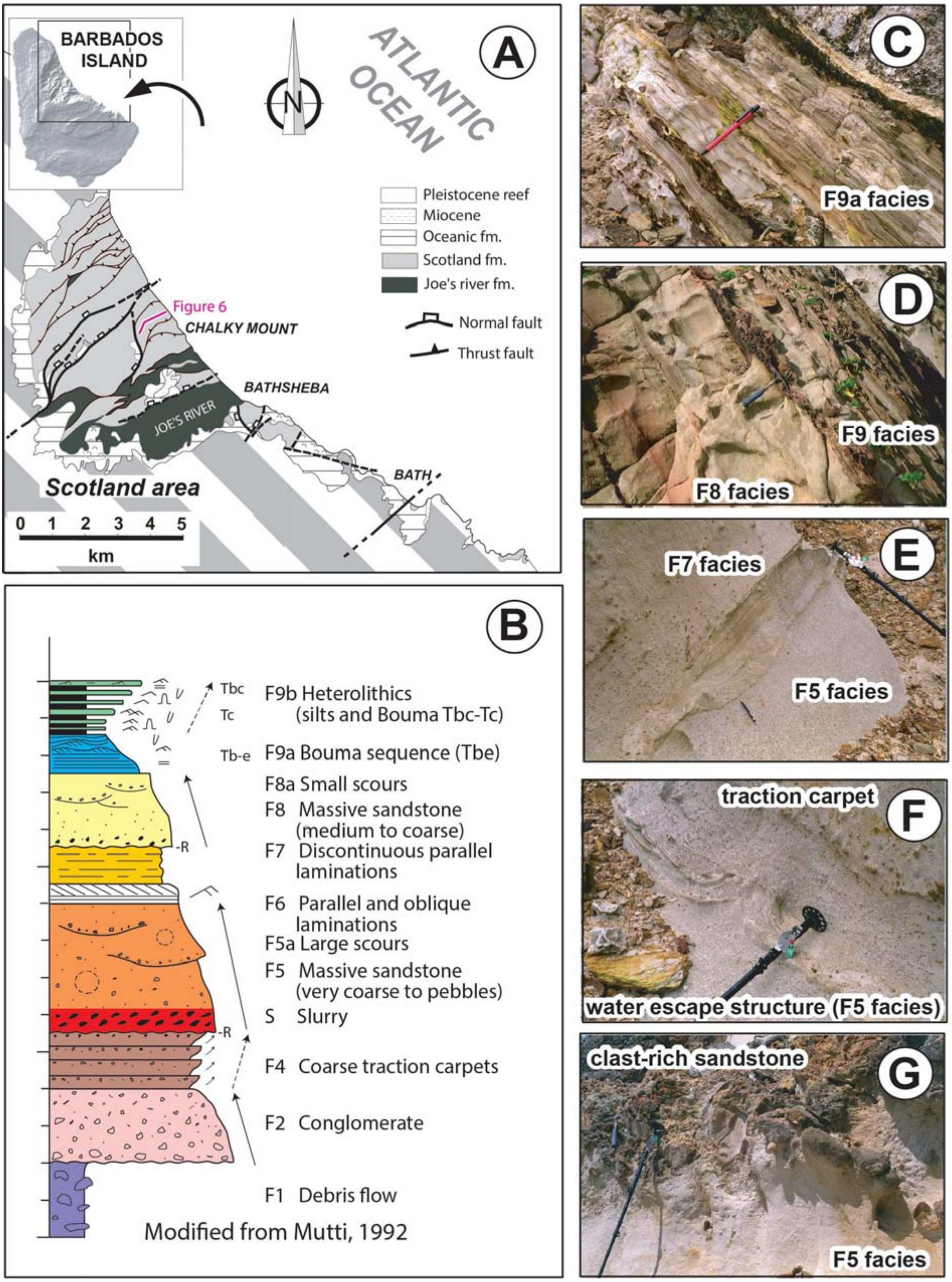

Figure 5 - The different sedimentary facies found in the turbidites outcropping at Chalky Mount, onshore Barbados Island. **A.** Structural sketch-map of the Scotland district and location of the crest of

Chalky Mount in Barbados island. **B.** Turbidite facies classification (Garcia et al., 2004) modified from Mutti (1992). The terms F4 to F9 are commonly recognized in the turbidite sequences (**C** to **G**).

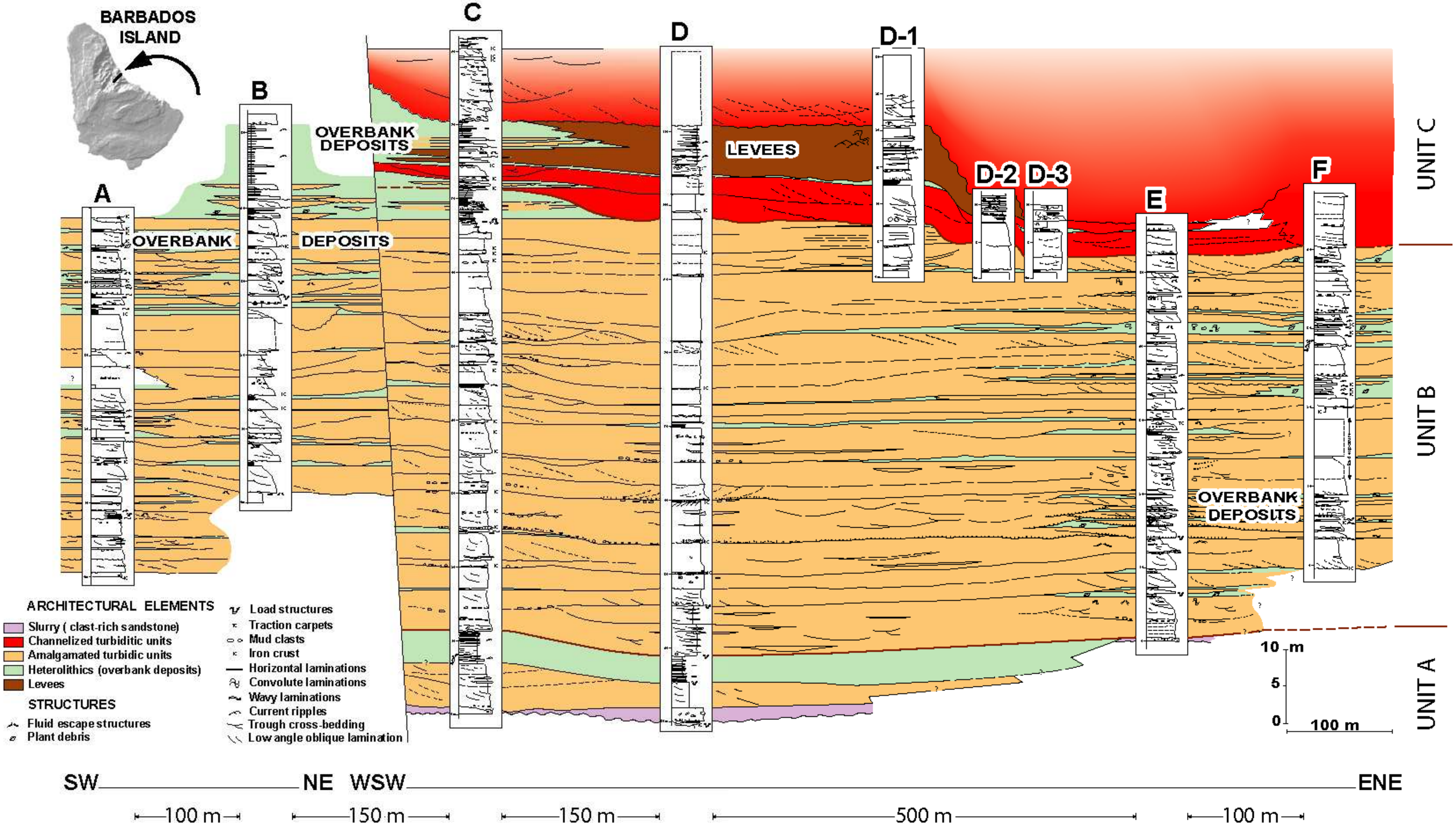
BARBADOS ISLAND
A
B
C
D
D-1
D-2
D-3
E
F
OVERBANK DEPOSITS
OVERBANK
DEPOSITS
LEVEES
OVERBANK DEPOSITS
UNIT C
UNIT B
UNIT A
10 m
5
0
100 m
ARCHITECTURAL ELEMENTS
Slurry (clast-rich sandstone)
Channelized turbiditic units
Amalgamated turbidic units
Heterolithics (overbank deposits)
Levees
STRUCTURES
Fluid escape structures
Plant debris
Load structures
Traction carpets
Mud clasts
Iron crust
Horizontal laminations
Convolute laminations
Wavy laminations
Current ripples
Trough cross-bedding
Low angle oblique lamination
SW
NE
WSW
ENE
100 m
150 m
150 m
500 m
100 m

Figure 6 - Architectural elements found in the turbidites outcropping at Chalky Mount, onshore Barbados Island. The deposition model proposed is a system of amalgamated turbidites for unit A, and B, and channelized turbidites for unit C; unit A and B being separated by an heterolithic level corresponding to the abandonment phase of unit A.

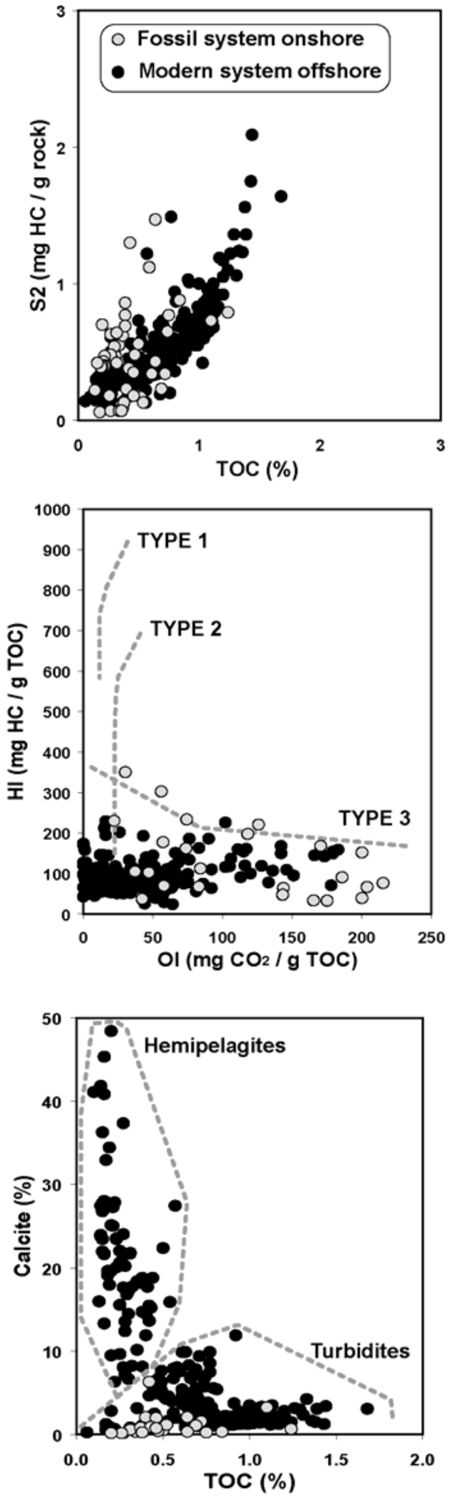

Figure 7 – Diagrams S2/TOC, HI/OI and Calcite/TOC compared between the fossil turbidite system onshore Barbados Island and the modern turbidite system. This notably shows the similar characteristics of the organic matter present in the fossil Eocene turbidite sediments onshore Barbados and the modern turbidite system offshore (TOC < 2%, S2 < 2 mg HC / g rock), with in both cases a type 3 organic matter (HI < 300 mg HC / g TOC) issued from terrestrial plan debris (see explanation in the text) and low calcium carbonate content in the organic-rich layers (< 10%).

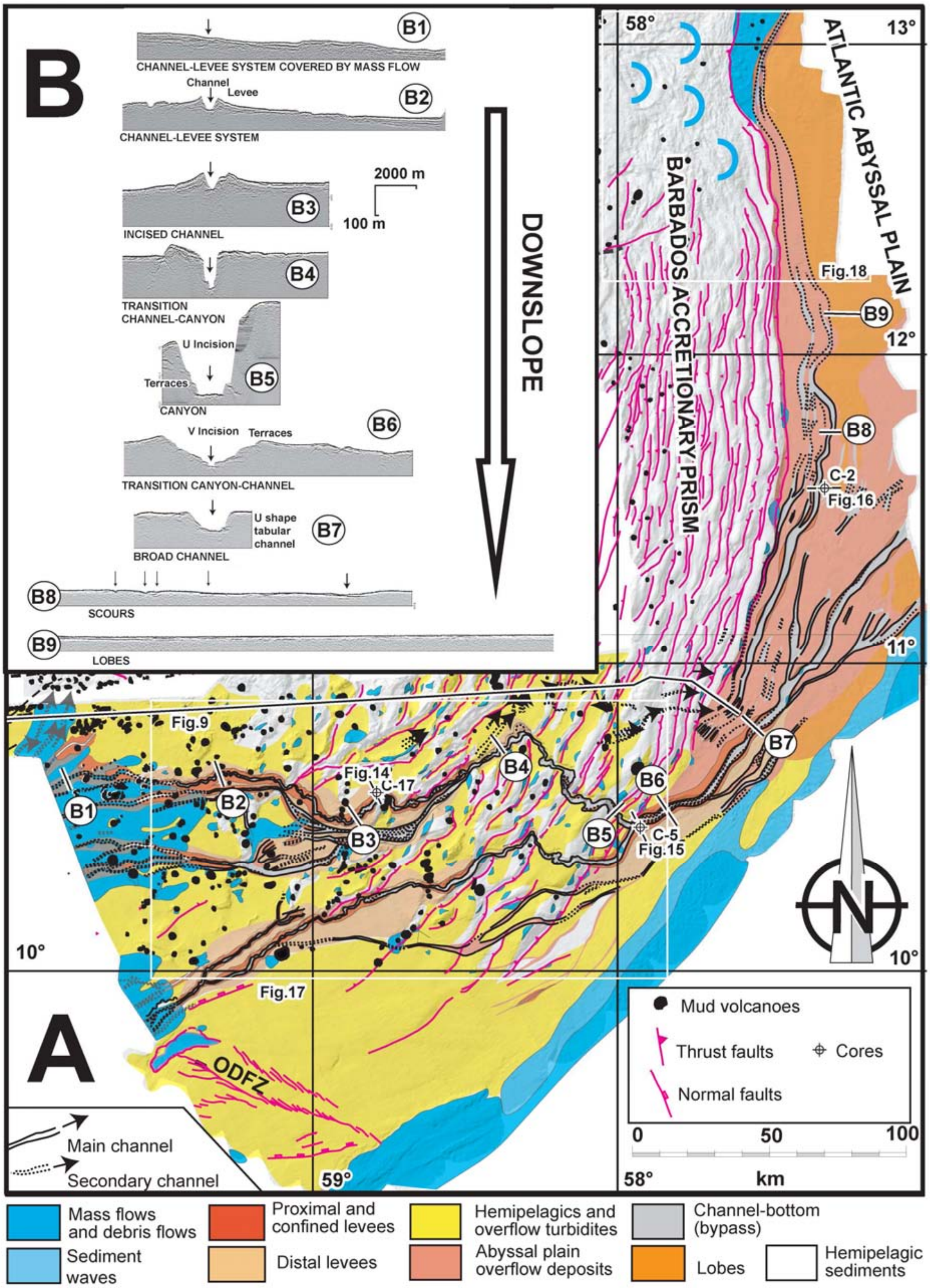

Figure 8 – A. Structural and geological map of relationship between the Orinoco turbidite system and the southern part of the Barbados accretionary prism (in white emergent structures of the Barbados

accretionary prism) with location of the cores of figure 14, 15, 16, and location of figures 9 17, 18; ODFZ: Orinoco delta fault zone (figure modified from Callec et al., 2009).

B. Evolution of the architecture of the turbidite channels along the Orinoco turbidite system (3.5 kHz profiles).

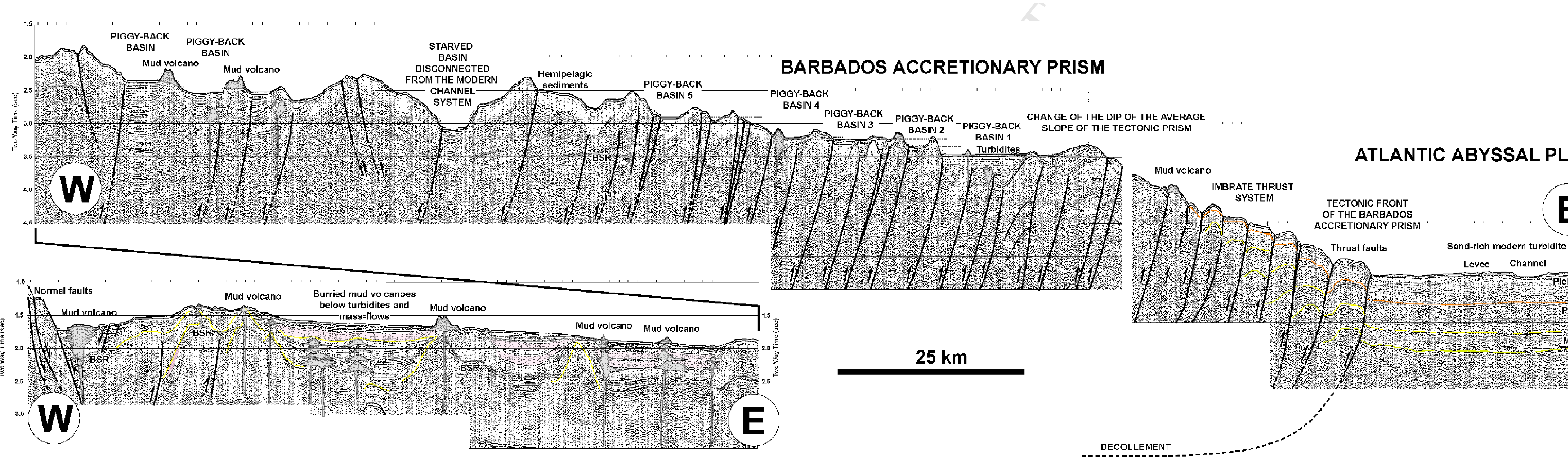
PIGGY-BACK BASIN
Mud volcano
PIGGY-BACK BASIN
Mud volcano
STARVED BASIN DISCONNECTED FROM THE MODERN CHANNEL SYSTEM
Hemipelagic sediments
PIGGY-BACK BASIN 5
BSR
BARBADOS ACCRETIONARY PRISM
PIGGY-BACK BASIN 4
PIGGY-BACK BASIN 3
PIGGY-BACK BASIN 2
PIGGY-BACK BASIN 1
Turbidites
CHANGE OF THE DIP OF THE AVERAGE SLOPE OF THE TECTONIC PRISM
ATLANTIC ABYSSAL PL
Mud volcano
IMBRATE THRUST SYSTEM
TECTONIC FRONT OF THE BARBADOS ACCRETIONARY PRISM
Thrust faults
Sand-rich modern turbidite
Levee
Channel
W
E
Two Way Time (sec)
Normal faults
Mud volcano
BSR
Mud volcano
Burried mud volcanoes below turbidites and mass-flows
Mud volcano
Mud volcano
Mud volcano
25 km
DECOLLEMENT

Figure 9 – Seismic transect across the southern part of the Barbados accretionary prism and the Atlantic abyssal plain. Light grey surfaces correspond to the main mud volcanoes and pink surfaces are transparent bodies that correspond partly to large-scale mass-flows. Dark grey lines show the main BSR. Yellow lines outline some good reflectors (with no specific interpretation).

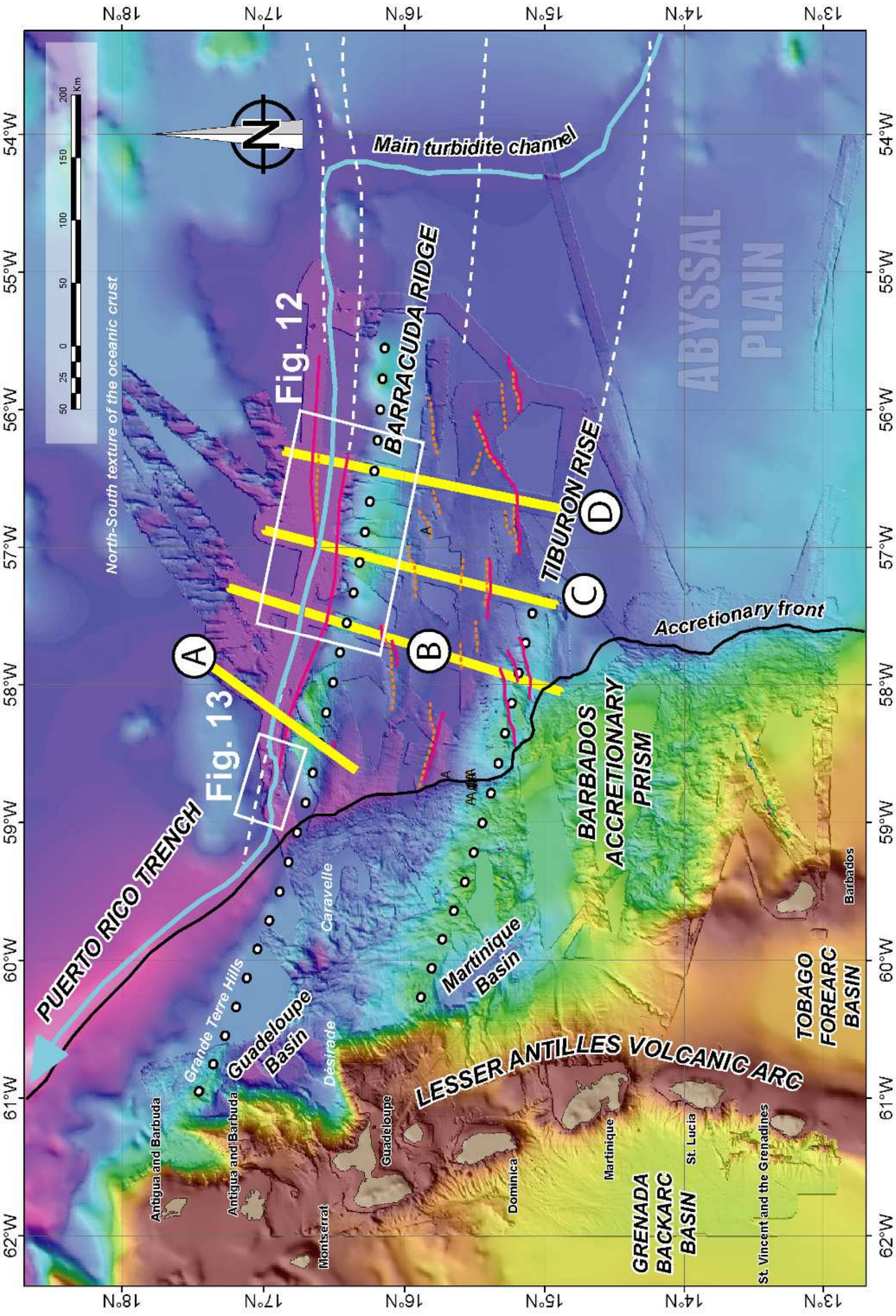

Figure 10 – Structural map showing the interaction between the Barbados accretionary prism and the distal turbidite system issued from the Orinoco delta in the plate boundary area between North America and South America and the northern part of the Barbados accretionary prism. The colour gradient of the topography ranges from light brown in the onshore areas to purple colours below 5500 meters of water depth. Red lines correspond to active faults which are visible at the sea bottom and dotted orange lines correspond to folds which are visible at the sea bottom. A-D are the locations of seismic lines shown in figure 11.

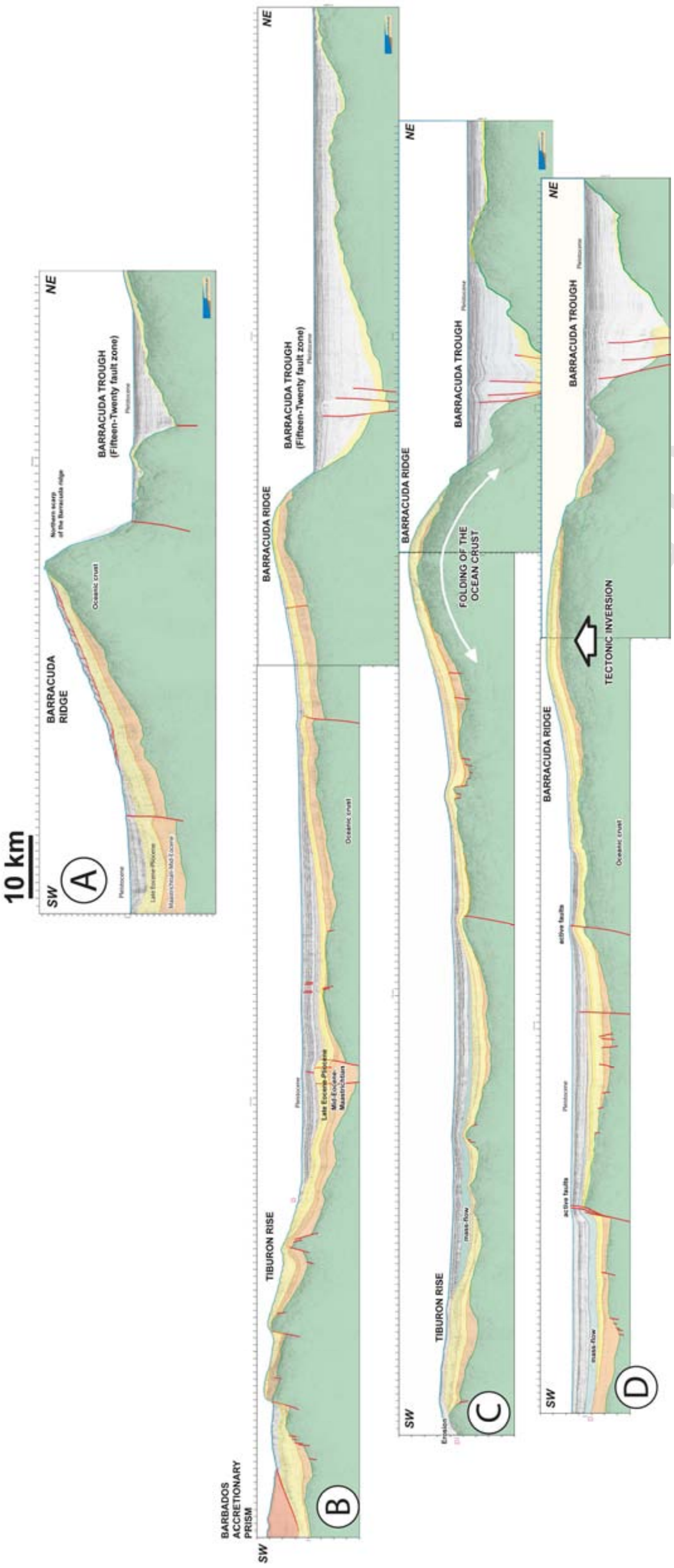

Figure 11 – Seismic lines illustrating the thickness and the deformation processes of the sedimentary pile in the plate boundary area between North America and South America, at the front of the northern part of the Barbados accretionary prism. Note the important thickness of the recent sediments (Late Pliocene-Quaternary) in the Barracuda trough. See figure 10 for locations of the seismic sections.

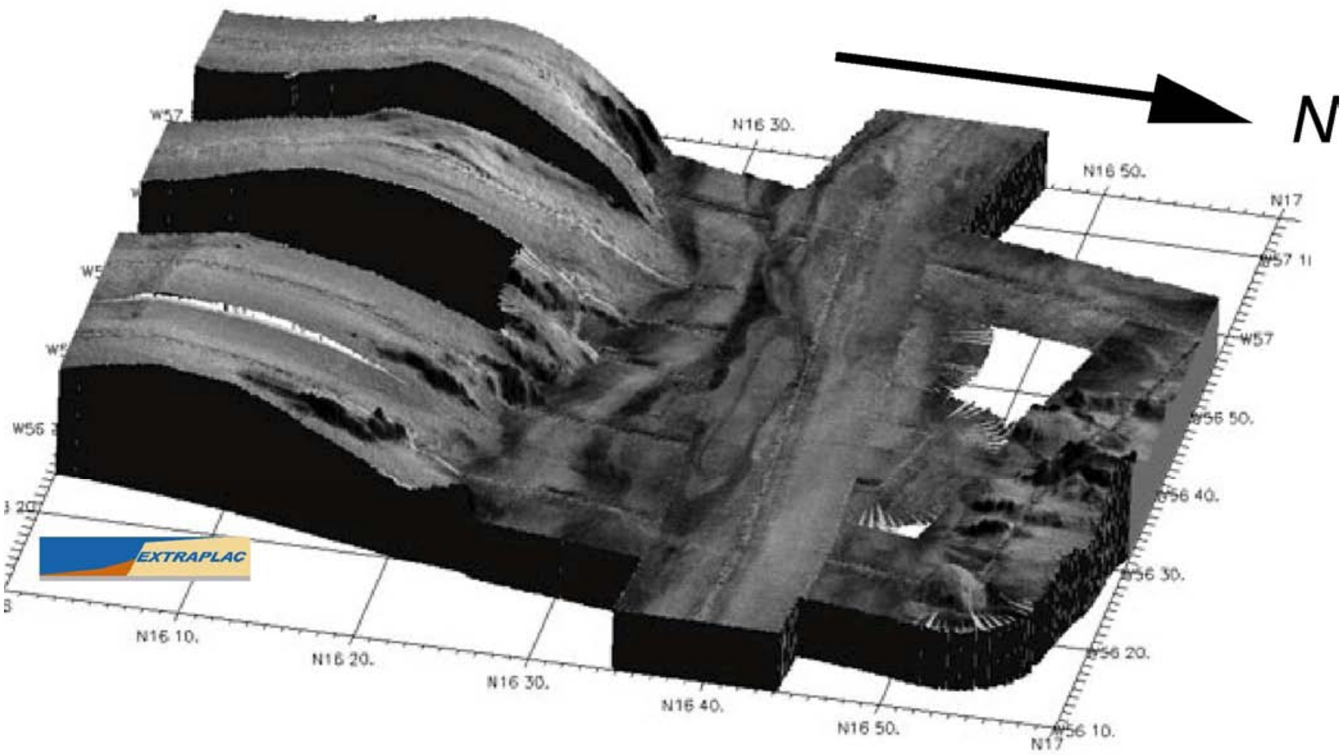

Figure 12 - Block diagram of seabed back-scattering imaging acquisition in the north of the Barracuda ridge and in the Barracuda trough. These data outline the low meandering geometry of the channels in the basin Barracuda.

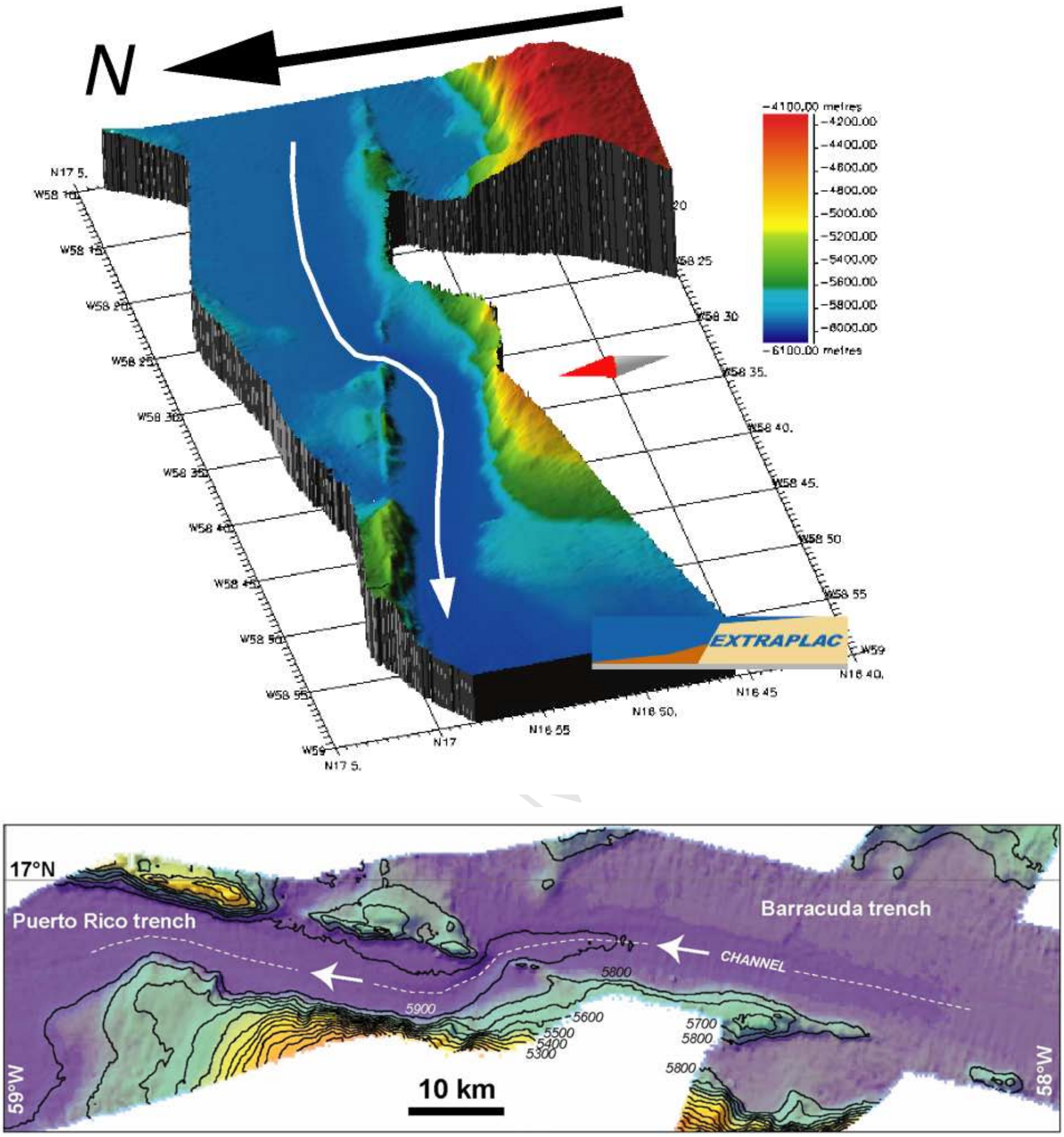

Figure 13 - Block diagram and bathymetric map showing (in white) the path of the main channel flowing from the Barracuda trough to the Puerto Rico trench in between a sub-linear volcanic ridge associated with the Fifteen-Twenty fracture zone (orange-yellow: above 5500 m of water depth, Green-blue: between 5500 and 5800 m, purple: below 5800 m).

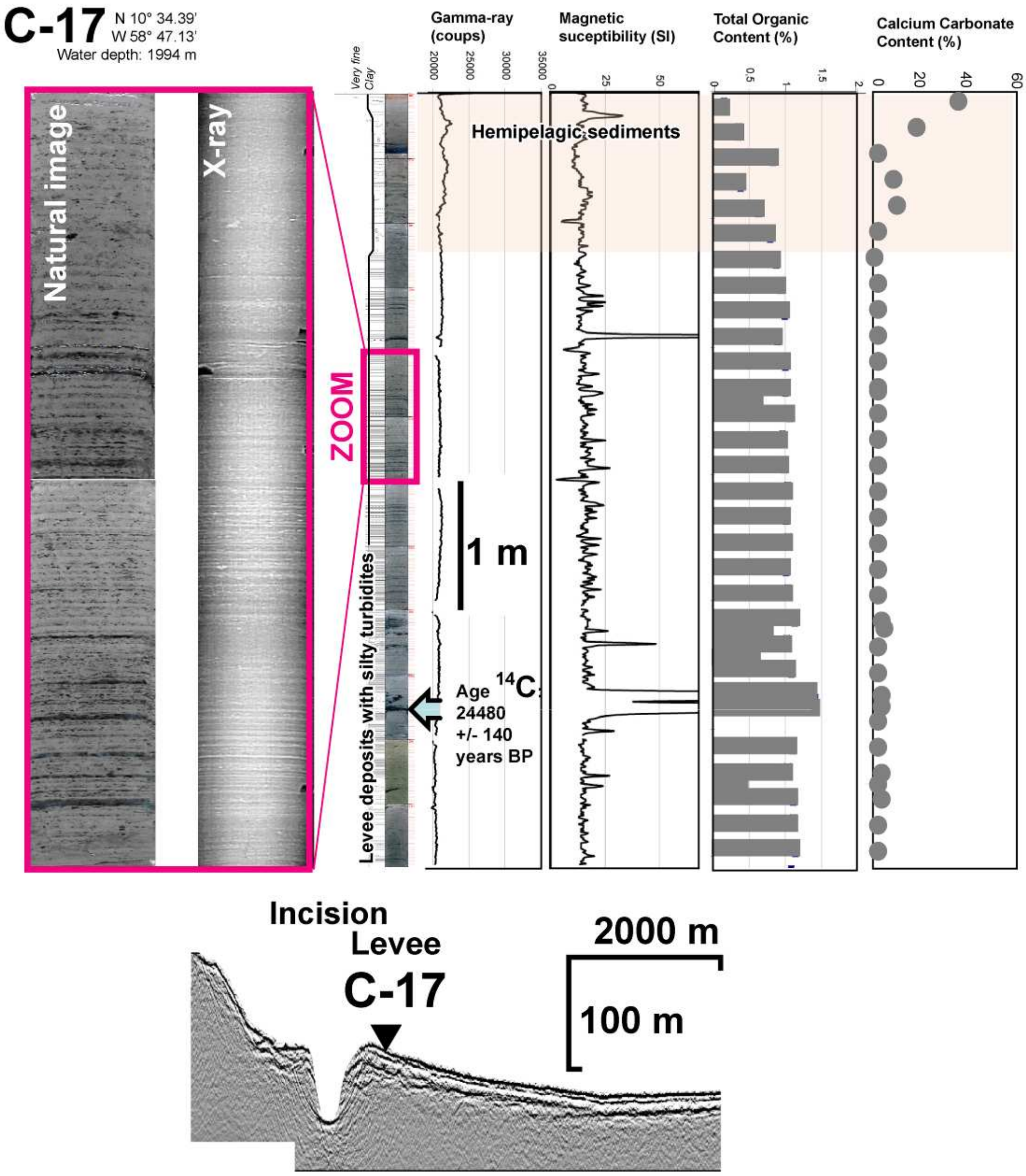

Figure 14 – An example of core collected on a levee of channel system in top of the Barbados accretionary prism (see location in figure 8), with gamma-ray attenuation, magnetic susceptibility, Total Organic Content characterization and calcium carbonate content. On the left part of this figure, a zoom of the natural image and X-Ray radiography of a part of the core is shown outlining that the levee deposits (including dark organic-rich levels) correspond to very fine silty turbidites. ^{14}C dating at the base of the core gave an age of 24480 +/- 140 year BP (last glacial period). Below is shown a 3.5 kHz section (echo-sounder) localizing where in the levee the core has been taken (map location in figure 8).

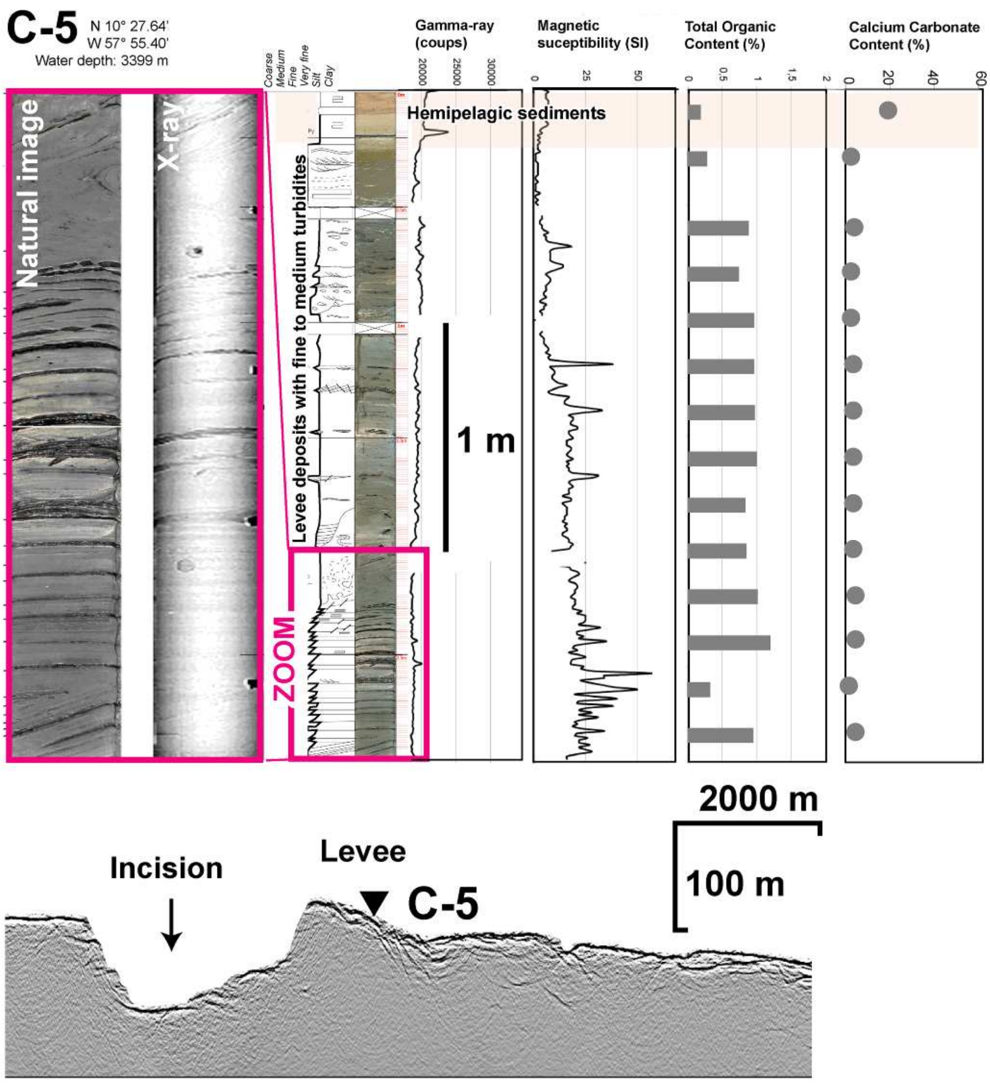

Figure 15 – An example of core collected on a high-relief levee of channel system in the abyssal plain immediately at the front of the Barbados accretionary prism (see location in figure 8), with gamma-ray attenuation, magnetic susceptibility, Total Organic Content characterization and calcium carbonate content. On the left part of this figure, a zoom of the natural image and X-Ray radiography of a part of the core is shown, outlining that on the levee dark organic-rich levels are interbedded with very fine silty turbidites. The sediments of the levee of the channel correspond to fine to medium turbidites. The upper most recent part of the sedimentation correspond to hemipelagic/pelagic deposits. Below is shown a 3.5 kHz section (echo-sounder) localizing where in the levee the core has been taken (map location in figure 8).

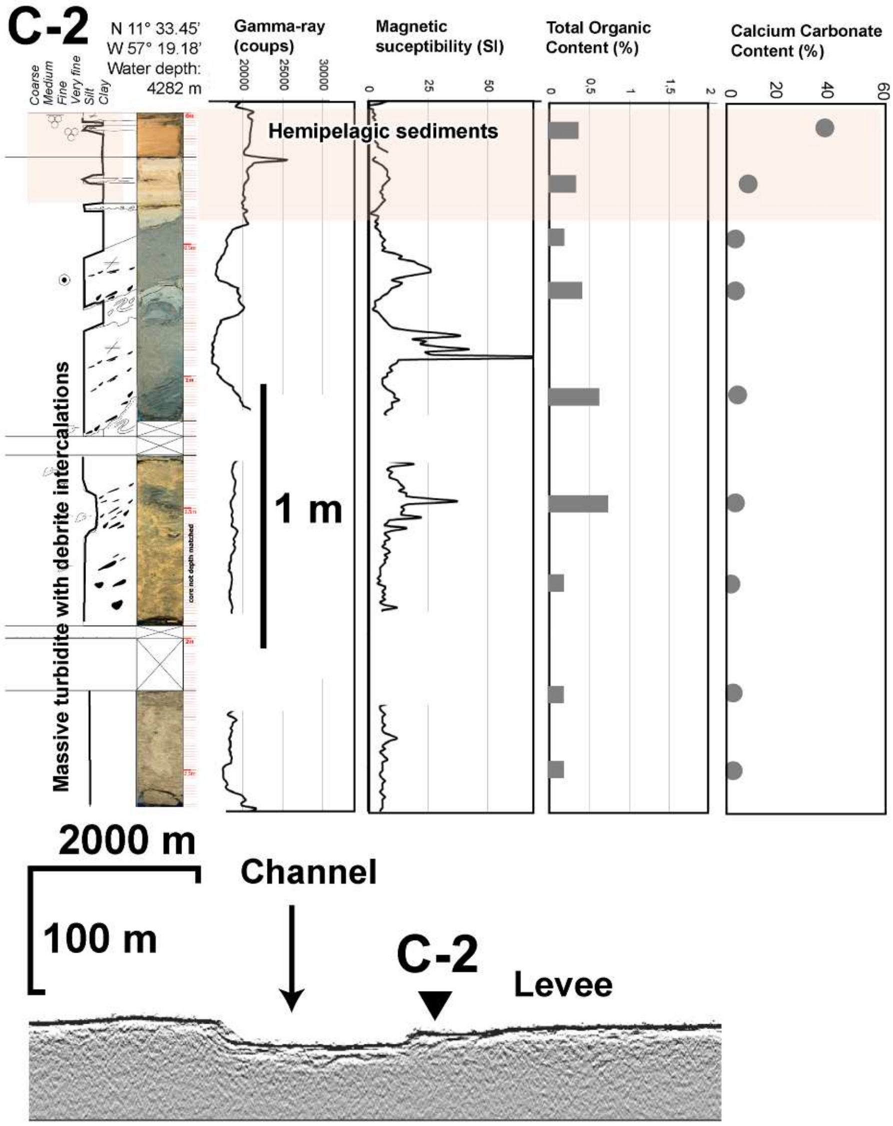

Figure 16 – An example of core collected on a low-relief overbank of the channel system in the abyssal plain about 20 kilometres east of the front of the Barbados accretionary prism (see location in figure 8), with gamma-ray attenuation, magnetic susceptibility, Total Organic Content characterization and calcium carbonate content. The sediments of the levee of the channel correspond to massive turbidites with debris intercalations. The upper most recent part of the sedimentation corresponds to hemipelagic/pelagic deposits. Below is shown a 3.5 kHz section (echo-sounder) localizing where in the levee the core has been taken (map location in figure 8).

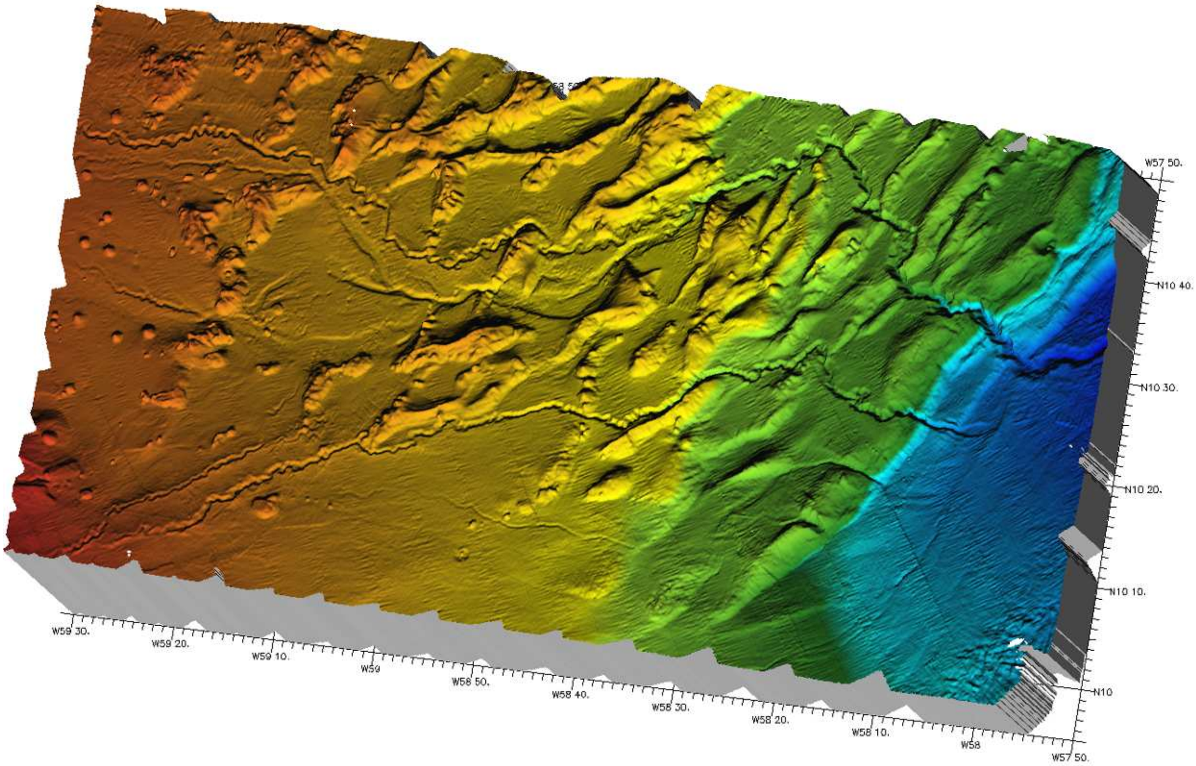

Figure 17 - Block-diagram from the EM12 multibeam acquisition showing the geometry of the channels and canyons of the Orinoco turbidite system on top of the tectonic front of the Barbados prism between 10°N and 11°N. The colour gradient of the topography ranges from above 800 m of water depth in red, to below 3000 m of water depth in blue.

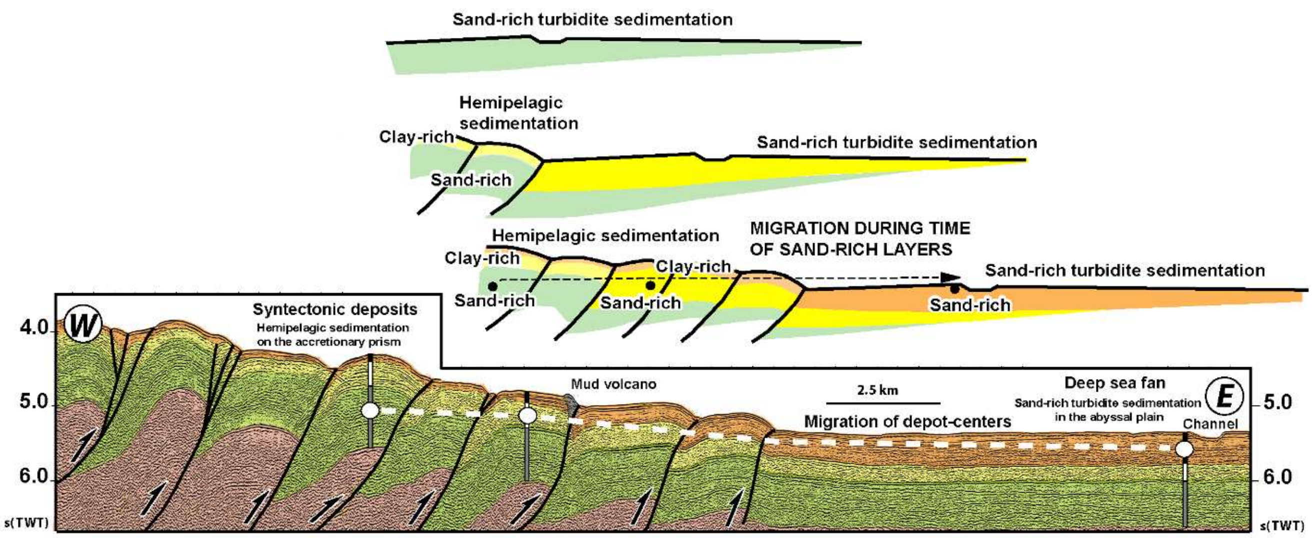

Figure 18 - An example of seismic line in the front of the accretionary prism, note the changes of thickness of the upper Quaternary levels with migration of the depocentres toward the abyssal plain during time (location of the profile in Figure 8). Note the migration of the maximum thickness of three characteristic seismo-stratigraphic sequences (dark green, light green and orange) outlined along 3 vertical lines (the white points correspond to the maximum thickness of each sequence). Above is proposed a conceptual model suggesting the progressive incorporation of abyssal plain thick sand-rich deposits inside the accretionary prism.

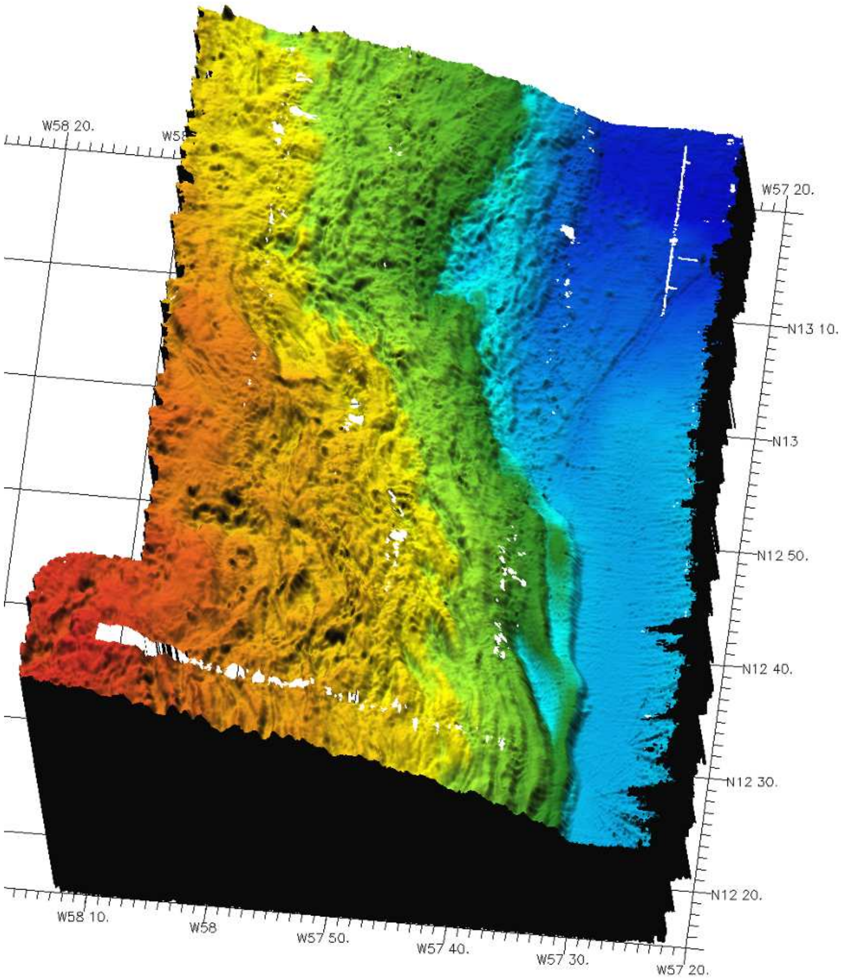

Figure 19 - Block-diagram from the EM12 multibeam acquisition showing the slope destabilization of the tectonic front of the Barbados prism in the area of 13°N (gigantic mass-flow). The colour gradient of the topography ranges from above 2500 m of water depth in red, to below 3800 m of water depth in blue.

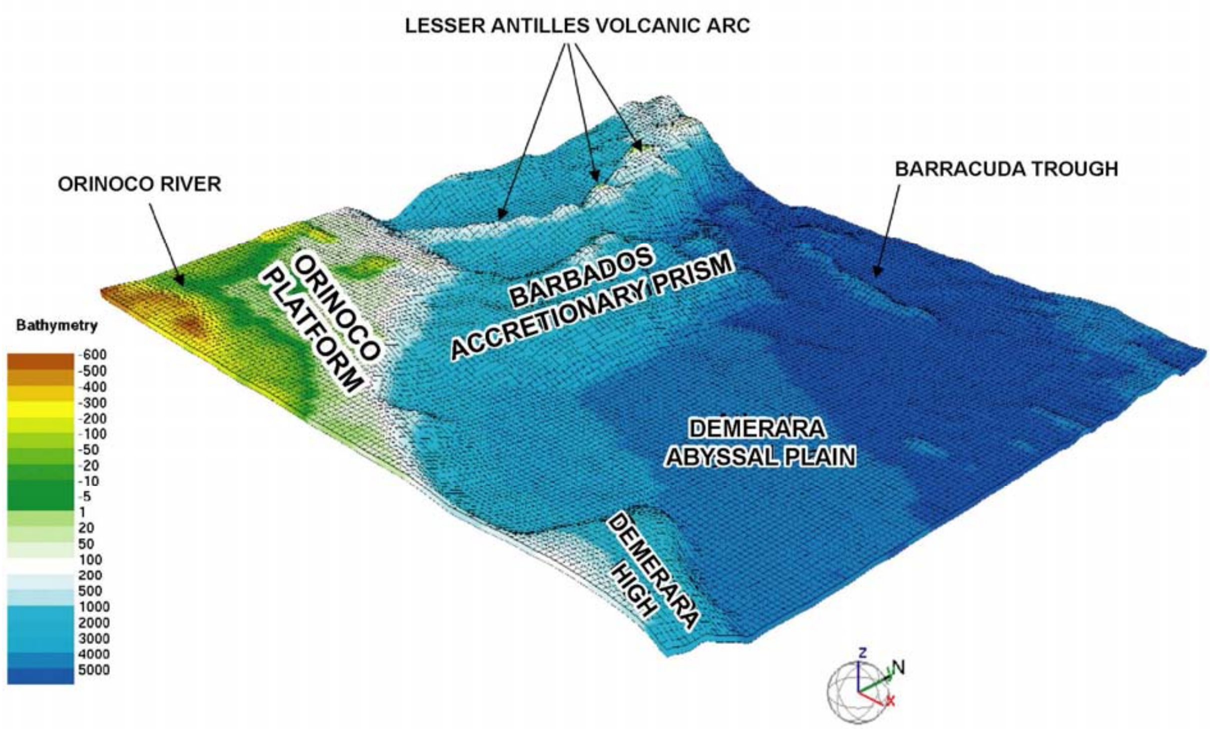

Figure 20 – The area covered by the stratigraphic modelling (1 200 x 1 200 km², vertical exaggeration x 20)

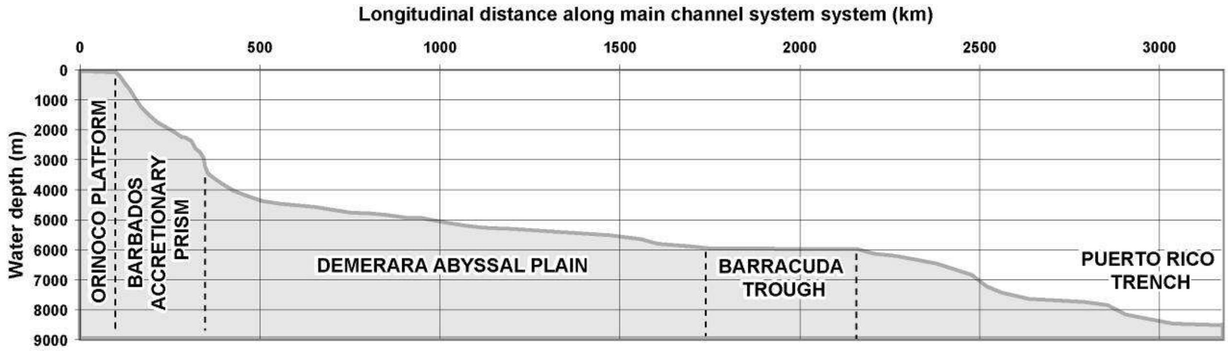

Figure 21 – Longitudinal bathymetric profile of the main offshore channel system of the Orinoco (data mixed from multibeam echosounder and satellite altimetry; Smith and Sandwell, 1997). Error bars are within the thickness of the line.

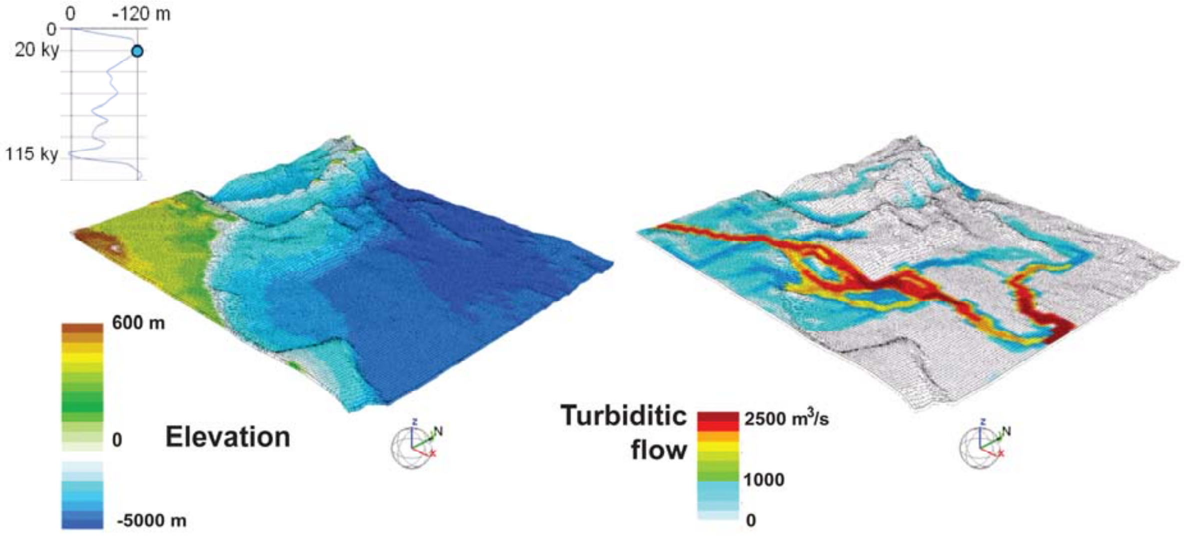

A

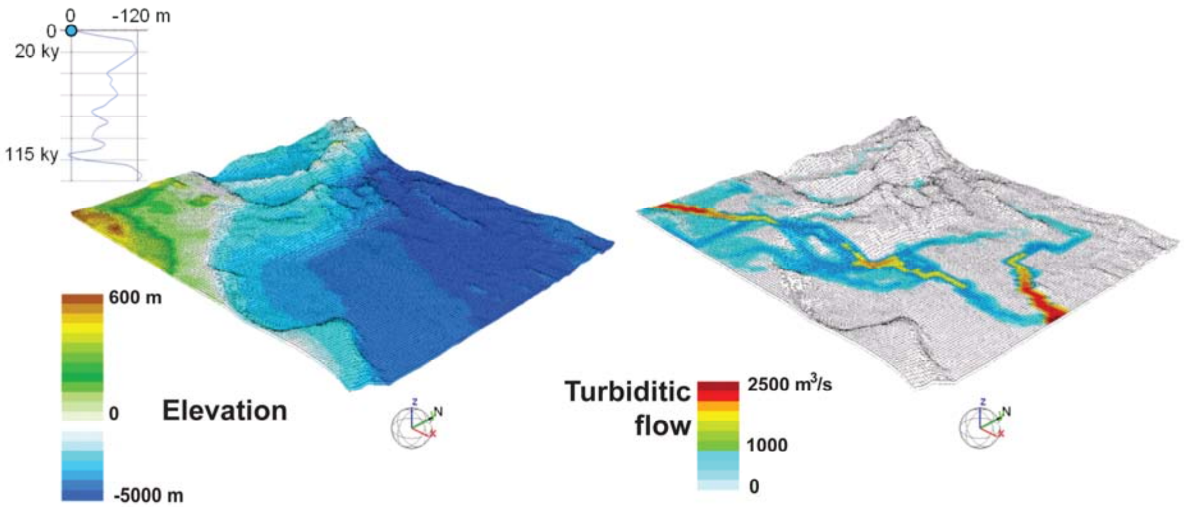

B

Figure 22 – Comparison of the modelling result at (**A**) 20 000 years (the lowest sea level), and Present (**B**)(the highest sea level). During the lowstand system, the Venezuelan shelf emerged and the Orinoco river directly fed a multiple-turbidite channel network, while during the highstand system, the shelf is flooded and water discharge dissipated, inducing a relative starvation of the deep-sea system.

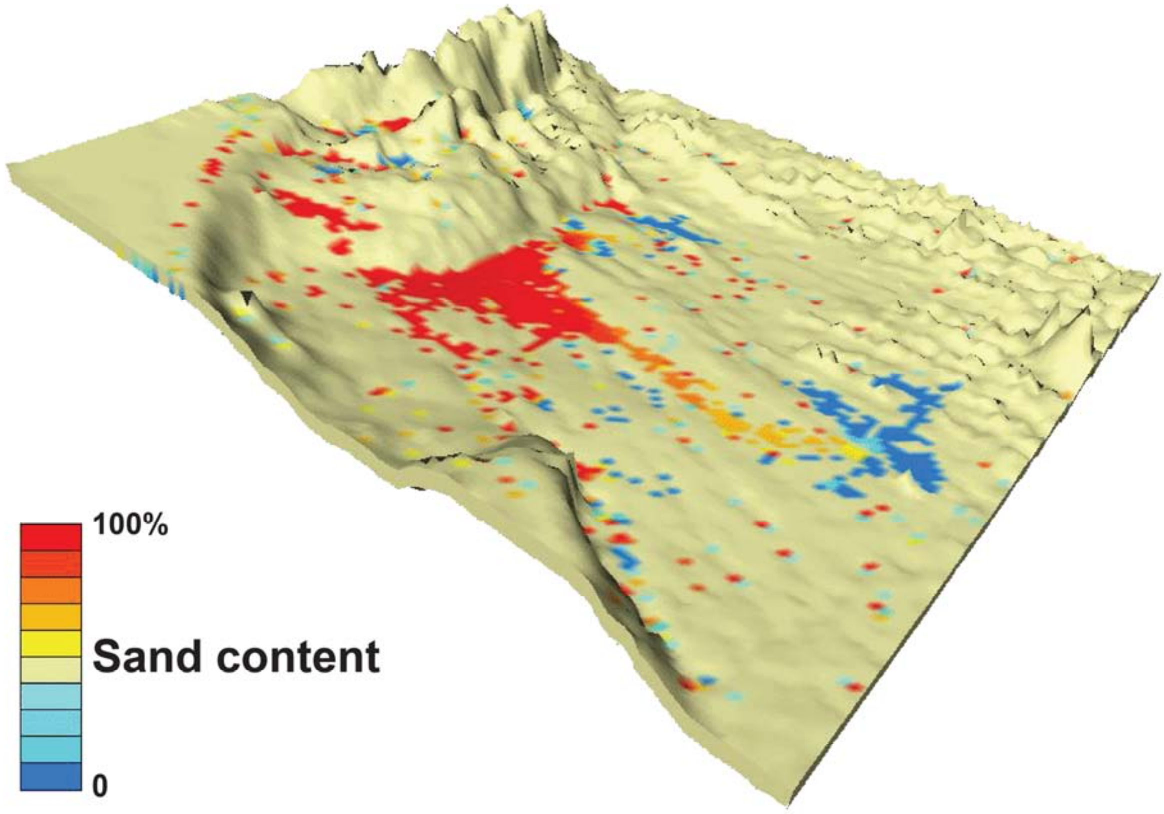

Figure 23 – Distribution of the sand content in the deposited turbidites in the simulation A of figure 22 (at 20 000 years, the lowest sea level). Turbidite sediments are rich in sand on top of the Barbados accretionary prism and in the abyssal plain at the front of the accretionary prism.

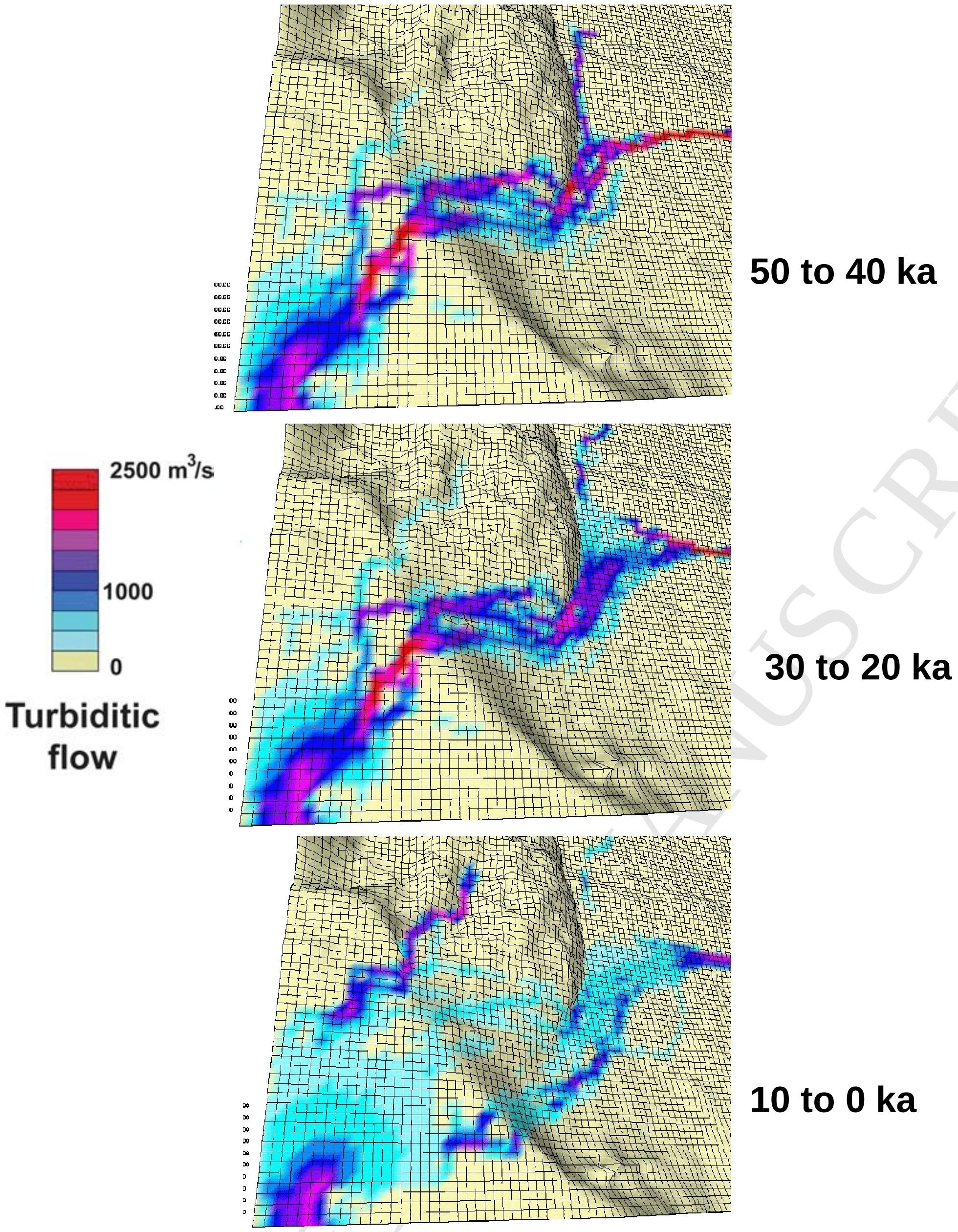

Figure 24 – Numerical modelling of the evolution of the turbidity currents during the last 50 ka on top of the Barbados accretionary prism (location corresponds to figure 25). High flows are observed during the lowstand period before 10 ka, and the flow is decreasing since the last glacial event.

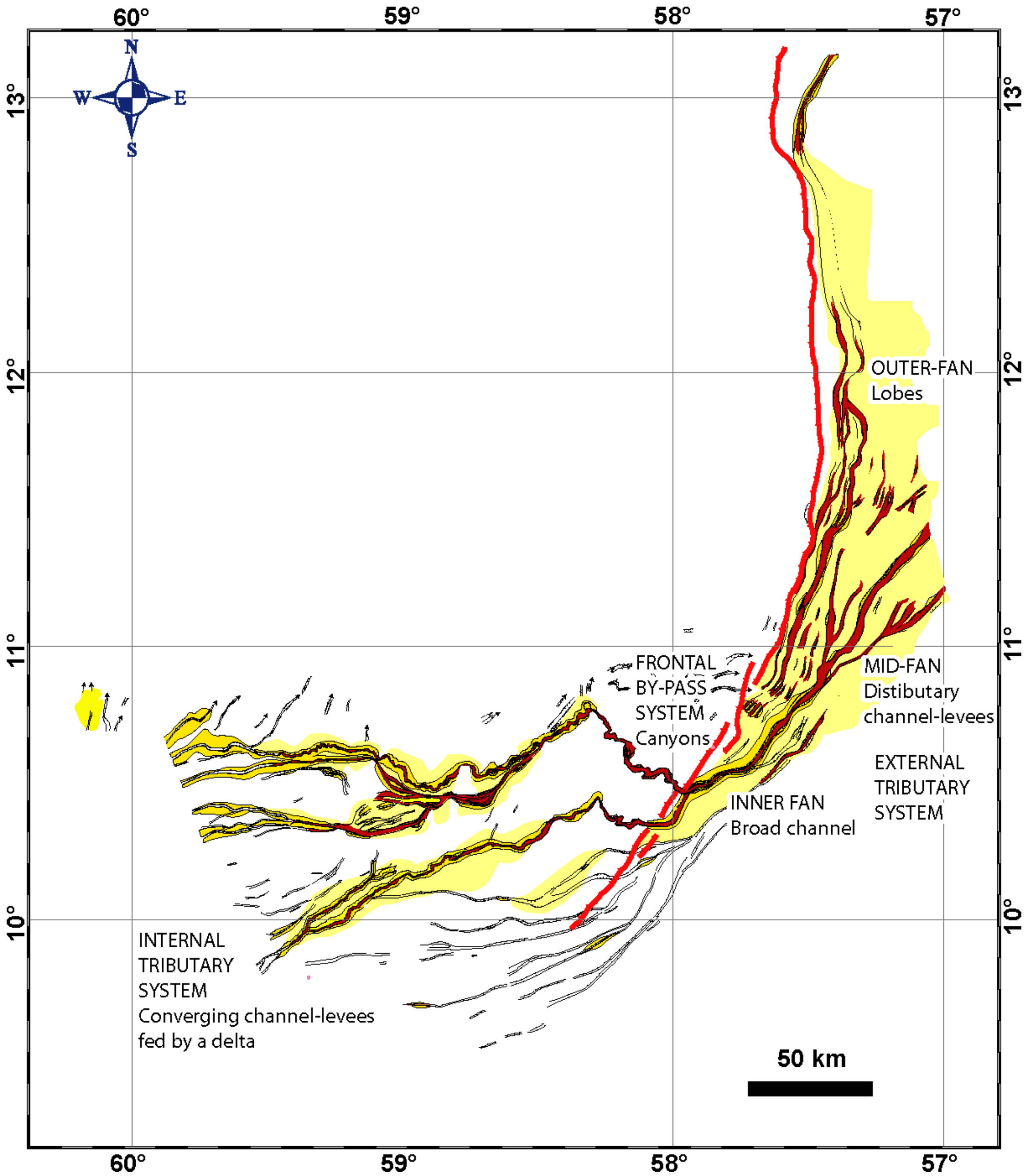

Figure 25 – Sketch-map of the organization of the Orinoco turbidite system in the interaction zone with the southern part of the Barbados accretionary prism (red: channels, dark yellow: levees, light yellow: overflow deposits and lobes). The light red line corresponds to the tectonic front of the accretionary wedge..

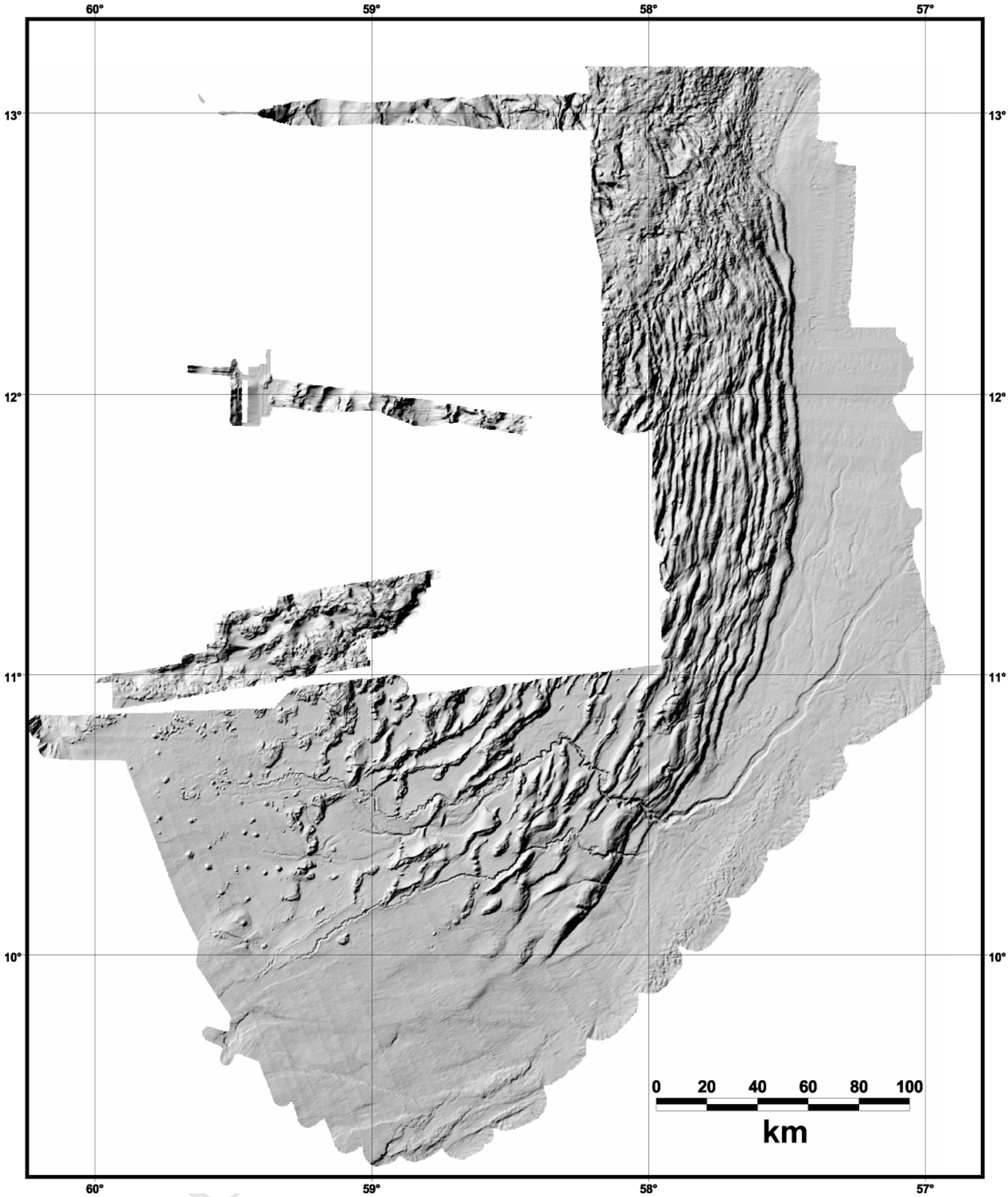

Accompanying digital Figure 1 – EM12 bathymetric map of the southern part of the Barbados accretionary prism. Note the channel pattern controled by the tectonic features of the accretionary prism.

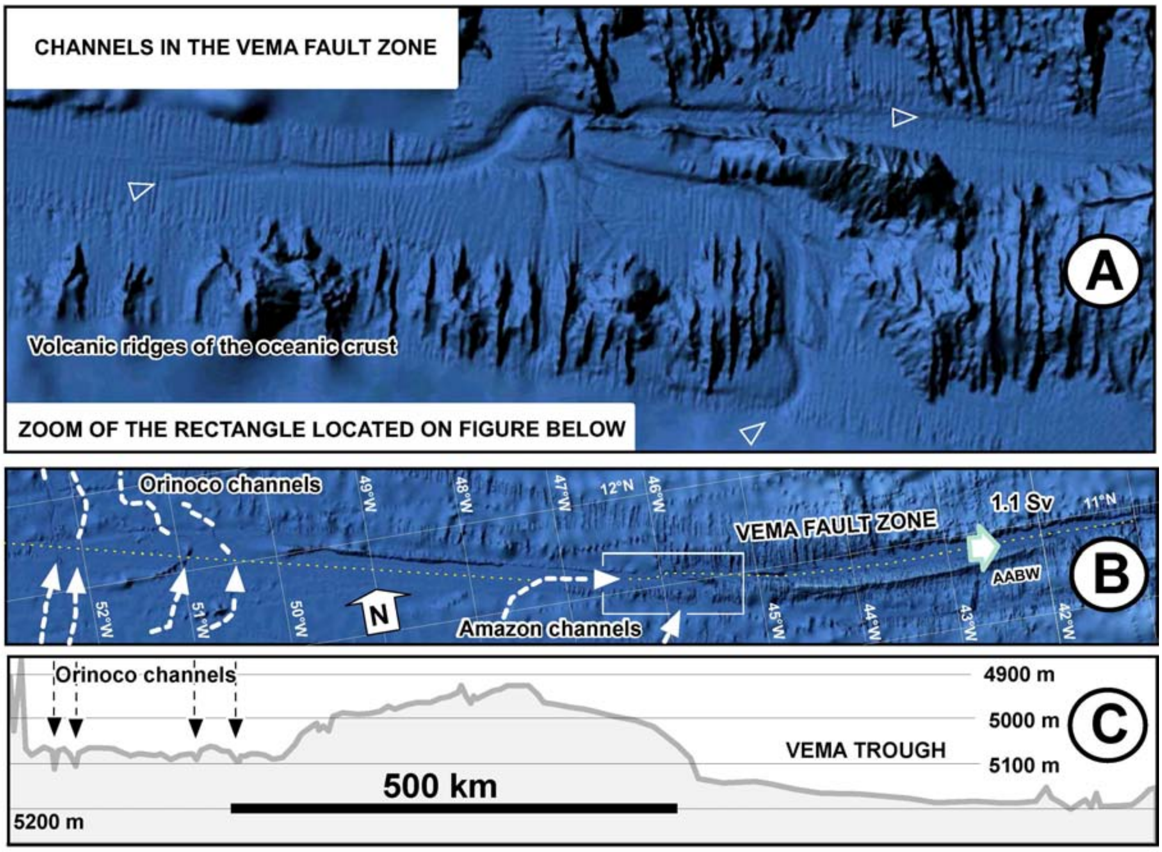

Accompanying digital Figure 2 – Detailed bathymetric map (A), and general bathymetric map (B) of the Vema fracture zone (Data SIO, NOAA, US Navy, GEBCO directly available on Google earth) and elevation profile (C) along the Vema fracture zone (Yellow dotted line on B). Note the eastward verging channel within the Vema fracture zone (locally with incision up to 150 m) consistent with the measured bottom current of 1.1 Sv (1.1 x 10^6 m^3/s) toward the east, which is assigned to be related to the connection of the Antarctic Bottom Water (AABW) with eastern Atlantic (Rhein et al., 1998).